Indian J. Phys. **82(10)** 1339-1371 (2008)

IJP

Fluctuation and fractal Characteristics of ring like and jet like events produced at SPS energies

Dipak Ghosh*, Argha Deb, Prabir Kumar Haldar[1] and Sima Guptaroy[2]
Nuclear and Particle Physics Research Centre, Department of Physics,
Jadavpur University, Kolkata-700 032, India
[1]Dinhata College, Coch Behar District, West Bengal, India
[2]Basanti Devi College, 147B Rashbehari Avenue, Kolkata-700 029, India

E-mail: dipakghosh_in@yahoo.com

Received 25 September 2006, accepted 30 May 2008

Abstract : We present here the study of pion fluctuation patterns in terms of Scaled Factorial Moments (SFMs) in one dimensional space (pseudorapidity and azimuthal angle) for ring like and jet like events in ^{32}S-AgBr interactions at 200 A GeV energy. The study reveals a clear signal of intermittency in the density fluctuations for both types of events. It is however observed that, strong intermittent pattern is revealed only in jet like events. The behaviors of anomalous fractal dimensions and generalized fractal dimensions reflect the self similar cascade mechanism. Moreover, the non-thermal phase transition is seen only in jet like events for pseudorapidity variable and in ring like events for azimuthal angle variable. The multifractal specific heats and entropy have also been calculated.

Keywords : Multifractality, generalized dimensions, non thermal phase transition, ultra-relativistic nucleus-nucleus collisions, intermittency, ring like events and jet like events.

PACS Nos. : 25.75.-q, 25.70.Mn, 24.60.Ky

1. Introduction

Ultra-relativistic heavy-ion collisions offer the unique opportunity to probe highly excited dense matter under controlled laboratory conditions. The studies of the multiplicity distribution of the produced hadrons and the analysis of the correlations among them play a fundamental role in extracting the details of the dynamics of the produced particles. The full-multiplicity distribution is a global characteristic and is influenced by conservation laws. On the other hand, the multiplicity distributions in restricted phase space domains contributing to the correlations are local characteristics and have an advantage of being much less affected by global conservation laws. The large

*Corresponding Author

fluctuation in the number of produced particles in local regions of phase space is one of the proposed signals for collective phenomena in relativistic nuclear interactions.

In the last decade, study of multiplicity distributions in limited regions (bins) has been used to probe for local dynamical fluctuations of an underlying self-similar (fractal) structure, the so-called intermittency phenomenon [1,2]. Bialas and Peschanski [3] introduced the method coined 'intermittency' from the field of fluid dynamics to analyze the data on high energy interactions in terms of scaled factorial moments (SFMs) as a function of decreasing rapidity intervals to search for non-statistical fluctuations. They suggested that if intermittency exists, then the normalized factorial moments of the multiplicity distribution should exhibit characteristic power law dependence $\langle F_q \rangle \propto M^{\alpha_q}$. M is the number of the bins, into which, the phase space of produced particles is divided, and α_q are the intermittency indices. The observation of intermittency may be due to the self-similar structures in random cascading for elementary processes or in nuclear collisions by the [4,5] second order phase transition from the quark gluon plasma to the final hadronic state. Intermittency has been observed in various experiments, for all types of reactions over a wide range of energies [6–15].

The concept of intermittency is in turn intimately connected to the fractal geometry of the underlying physical process. Fractal geometry was developed from Benoit Mandelbrot's [16] study of complexity and chaos. The term *fractal* was coined in 1975 by Mandelbrot, from the Latin *fractus,* meaning "broken" or "fractured." This branch of mathematics is concerned with irregular patterns made of parts that are in some way similar to the whole, *e.g.* twigs and tree branches, a property called self-similarity or self-symmetry. The object need not exhibit exactly the same structure at all scales, but the same "type" of structures must appear on all scales. The most notable property of fractals is their dimension. Unlike conventional geometry, which is concerned with regular shapes and whole-number dimensions, such as lines (one-dimensional) and cones (three-dimensional), fractal geometry deals with shapes found in nature that have non-integer, or fractal dimensions – linelike rivers with a fractal dimension of about 1.2 and conelike mountains with a fractal dimension between 2 and 3. Deterministic chaos in nonlinear physics has been well explained in terms of fractal measures, [16]. The existence of self similarity property in high energy collisions implies that the ideas of deterministic chaos in nonlinear physics can be applied to analyze the data of high energy collisions. A formulation for treating fractal dimensions and its generalization has been developed [17,18] and successfully applied to the study of intermittent behavior in turbulent fluids and other transitions to chaos. This prompted exploration of intermittency in multiparticle production in terms of the multifractal formalism of fractal properties in multifractal production processes. The intermittency indices α_q characterize (multi) fractal structure of the distribution. Lipa [19] pointed out that the scaling property could be reinterpreted in terms of the fractal properties of the particle density fluctuation. It is possible to correlate the intermittency exponent α_q to

the generalized dimension, which is called Renye dimension [18], by $d_q = \alpha_q/(q-1) = 1 - D_q$, where d_q is the anomalous fractal dimension or Renyi co-dimension and measures the intermittency dimension. D_q is the generalized fractal dimension which describes fractal and multifractal in the classical system. It is important to study q dependence of D_q as it points out the possible mechanism of multiparticle production process [18]. Also, it reflects the inner fractal structure of the fluctuations representing monofractal pattern with the unique D_q, or multifractal ones with the hierarchy $D_{q1}\langle D_{q2}, q_1\rangle q_2$ [20].

The signal, whether a phase transition has been taking place, is the most intriguing question in the study of high-energy interaction. Phase transition may be of thermal or of non-thermal type, depending on whether the new phase is characterized by new thermal behaviour or not. If a quark-gluon-plasma is formed in thermodynamic equilibrium during a high-energy interaction, then a possible phase transition to the final hadronic phase should follow it. If this phase transition is sufficiently close to the second order, then the final hadronic phase is expected to show intermittent behaviour. In that case, fractal co-dimension, d_q, is expected to behave independently of the order of the moment q. Otherwise, if the phase transition is of first order with short correlation length, then final hadronic phase is no longer self-similar at large scales. In that case, the fractal co-dimension should vanish. On the other hand, if self-similarity is the underlying mechanism of particle production, then fractal co-dimension d_q should depend on the order of the moment q. Thus, monofractal patterns [d_q = const. (q)] are associated with second-order phase transition (*e.g.* from quark-gluon plasma), while self-similar cascading is characterized by multifractals $\left[d_{q1} > d_{q2}, \text{ at } q_1 > q_2\right]$ with a possible "non-thermal" phase transition. However, the parameters of the self-similar cascade can be chosen in such a way that fractal co-dimension will become independent of q [21]. So, the condition d_q = constant, is not sufficient to ensure that a phase transition has taken place.

Non-thermal phase transition leads to the co-existence of different phases in analogy with different phase spin-glass system. Peschanski [22] observed that if intermitency is due to self-similar cascading, then a non-thermal phase transition might take place. Peschanski and Bialas observed that if two phases co-exist, then the function defined by $\lambda_q = (\alpha_q + 1)/q$ should have a minimum at a certain value $q = q_c$. The minimum of λ_q may be also a manifistation of coexistence of (many small) liquid-type fluctuations and dust-type (high density) ones. It has been shown in different works that self-similar multiparticle systems behave differently in the regions $q < q_c$ and $q > q_c$ [20]. It has been conjectured that the region $q < q_c$ appears to be dominated by numerous fluctuations containing not much more than q_c particles in one bin. The region $q > q_c$ is governed sometimes by a small or very large fluctuation. This situation resembles a mixture of a "liquid" of many small fluctuations and a "dust" consisting of a few grains of very high density. The "liquid" and the "dust" coexist. When the system

is probed by a moment of rank $q < q_c$ one sees only the liquid phase. When the system is probed by a moment of $q > q_c$ one sees only the dust exist phase. Different data sets of varying projectile nature and energy have already been utilized to search for non-thermal phase transition.

From an analysis of azimuthal distribution of pions in ultra-relativistic nuclear collisions two different classes of substructures are found which are referred as jet like and ring like structures [23]. The ring-like structures are occurring where many pions are produced in a narrow region along the rapidity axis which are at the same time diluted over whole azimuth. On the other hand, the jet like structure consists of cases where particles are focused in both dimensions [24]. The ring-like events have been reported in cosmic rays [25–28] long ago and then subsequently in accelerator energy in nucleus-nucleus collisions [29,30]. The origin of ring like events is still unknown. It has been suggested [29,31–38] that similar to electromagnetic forces, strong interactions might induce coherent collective effects in hadronic matter which result in the so-called ring-like events. The analogue to Cherenkov-photons would be Cherenkov-gluons emitted by a parton (quark) entering a hadronic medium. One can able to study the value of the nuclear index of refraction in nuclear matter from the cone angle of emission of gluons. Thus it is important to analyze these events in details. Although primarily it is observed that jet like and ring like events do not exhibit significant deviations from what can be expected from stochastic nature. But it is important to realize that the average values studies do not give full information of the process involved. Following the works of Adamovich *et al* [23], we have obtained ring-like and jet-like events in ^{32}S-AgBr interaction at 200 A GeV.

This paper presents a study of the non-statistical fluctuations in terms of scaled factorial moments in the pseudorapidity (η) and azimuthal (ϕ) angle distribution of pions in ^{32}S-AgBr interaction at 200 A GeV for ring like and jet like events separately. Here we investigate the variation of factorial moment with respect to decreasing phase space, which in turn, is closely related to the intermittent parameter α_q. The intermittency indices characterize (multi)fractal structure of the distribution. Fractal aspects in the pseudorapidity (η) and azimuthal (ϕ) angle space is studied for both events *via* the generalized fractal dimension D_q. We search for possibility of occurrence of non-thermal phase transition for both the events in terms of function λ_q. Bershadskii reported that the constant specific heat approximation (CSH), which is widely applicable in ordinary thermodynamics, is also applicable to the multifractal data. Following Bershadskii, we have determined the multifractal specific heat for ring like and jet like events in η-space and ϕ-space. We have also calculated the entropy function for jet like events.

2. Experimental details

The data used in the present investigation have been obtained from sets of photo

emulsion plates exposed to a ^{32}S beam with energy 200 A GeV at the CERN SPS. Here we are dealing with nuclear emulsion detector which is itself the target for any high energy projectile beam. A Leitz Metaloplan microscope with a 10× objective and 10× ocular lens provided with a semi-automatic scanning stage is used to scan the plates. To increase the scanning efficiency each plate is scanned by two independent observers. The final measurements are done using an oil-immersion 100× objective. The microscope employed for the measurement had a resolution of 1 μm along the x and y-axes and 0.5 μm along the z-axis (shrinkage factor being 2.5).

Each interaction was scanned using the "along-the-track" method with the help of a microscope. To reduce the loss of tracks as well as to reduce the error in angle measurement, we excluded events that occurred within 20 μm from the top or bottom surface of the pellicle. Great care was taken in the identification of different tracks.

After scanning, the events are chosen according to the emulsion terminology as :

Black particles : Black particles consist of both single and multiple charged fragments. They are target fragments of various nuclei like carbon, lithium, beryllium *etc.* with ionization greater or equal to $10I_0$, I_0 being the minimum ionization of a singly charged particle. Range of them is less than 3 mm. They have velocities less than $0.3c$ [c is the velocity of light in vacuum].

Grey particles : They are mainly fast target recoil protons with energy up to 400 MeV. They have ionization $1.4\,I_0 \leq I \leq 10I_0$. Their ranges are greater than 3 mm and having velocities $0.7c \geq V \geq 0.3c$.

Shower particles : The relativistic shower tracks with ionization I less than or equal to $1.4\,I_0$ are mainly produced by pions and are not generally confined within the emulsion pellicle. These shower particles have energy in GeV range.

The projectile fragments are a different class of tracks with constant ionization, long range and small emission angle.

For the present study we have chosen events without any observable projectile fragment and with the number of target fragments (black + grey) being larger than seven. These events are central collisions of the given beams with AgBr nuclei. According to the above selection procedure we had chosen 140 events of ^{32}S-AgBr interactions at 200 A GeV. The shower tracks numbered 12,133. The emission angle θ and azimuthal angle (ϕ) is measured for each track with respect to the beam direction by taking readings of the coordinates of the interaction point (X_0, Y_0, Z_0), coordinates (X_1, Y_1, Z_1) at the end of the linear portion of each secondary track, and coordinate (X_i, Y_i, Z_i) of a point on the incident beam. To study the scale dependence of fluctuations of observed shower particles, we have used the variable pseudorapidity, which is defined as $\eta = -\ln(\tan\theta/2)$, where θ is the emission angle with respect to

the beam direction. For emulsion stacks with exposures parallel to the emulsion plates, the uncertainty in the measurement of the emission angles, which is very essential for this study never exceeds a few mrad corresponding to a resolution of 0.1 units in pseudorapidity. For studying the density fluctuations, we vary the pseudorapidity range to $\Delta\eta = -3$ to $+7$. The azimuthal angle varies from $\Delta\varphi = 0 - 2\pi$.

3. Methodology for separation of ring like and jet like events

Each consecutive n_d-tuple of particles along the η-axis can then be considered as a group characterized by $\Delta\eta_c$ *and* $\rho_c = n_d/\Delta\eta_c$. Dense group can then be defined and recorded as above. This method has the advantage that all groups, including the discarded, more dilute ones, have by definition the same multiplicity n_d, and can be readily compared. With this method it is also a fairly simple task to compare the obtained sample with samples obtained by a purely stochastic process as well as samples obtained from model-based Monte Carlo calculations.

Next we need to parameterize the azimuthal structure in a suitable way, so that large values of the parameter represent one type of structure and small values the other. Two sums have been suggested as such parameters and are given by

$$S_1 = -\sum \ln(\Delta\phi_i)$$

and

$$S_2 = \sum (\Delta\phi_i)^2$$

where $\Delta\phi_i$ is the azimuthal difference between two neighbouring particles in the group. For the sake of simplicity, we can count $\Delta\phi_i$ in units of full revolutions and thus we have

$$\sum (\Delta\phi_i) = 1$$

Both these parameters will be large ($S_1 \to \infty$, $S_2 \to 1$) for jet like structures and small ($S_1 \to n_d \ln n_d, S_2 \to 1/n_d$) for ring–like structures.

In the present investigation we separate ring like and jet like events with the help of the parameter S_2. Figure 1 shows the $S/\langle S\rangle$ distribution for our data of ^{32}S-AgBr data at 200 A GeV. The distribution shows a peak at $S/\langle S\rangle = 0.6$. We consider ring like structured events having $S/\langle S\rangle < 1$ (0.3 to 0.7). The events having $S/\langle S\rangle$ around 1.2 are taken as jet like structure events.

4. Scaled factorial moment method

We consider the phase space interval ΔX be divided into M bins of size $\delta X = \Delta X/M$. The normalized factorial moment F_q of order q is defined as [39]

$$F_q(\delta X) = M^{q-1} \sum_{m=1}^{M} \frac{n_m(q_m - 1).....(n_m - q + 1)}{\langle n_m \rangle^q}, \qquad (1)$$

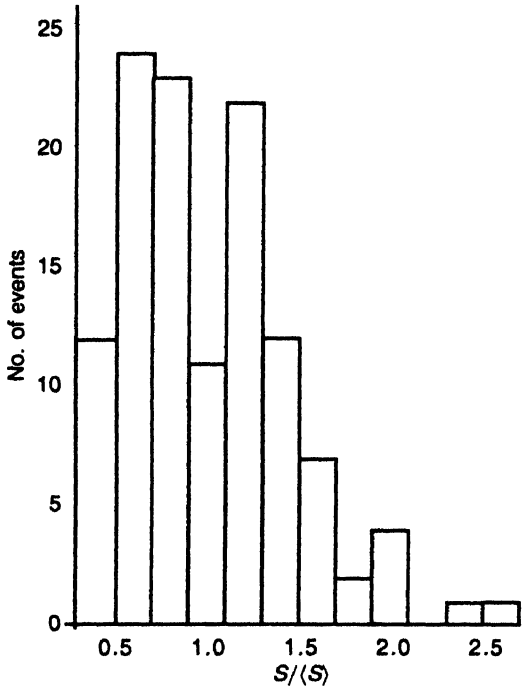

Figure 1. $S/\langle S\rangle$ distribution for pion data of ^{32}S-AgBr data at 200 A GeV.

where, n_m is the multiplicity in the m-th bin $\langle..\rangle$ indicates average over the whole sample of events. For given q and M values, F_q's are calculated for all the events and then averaged over the whole sample of events to obtain $<F_q>$. The most outstanding feature of this moment is that it can detect and characterize the non-statistical density fluctuations in particle spectra, which are intimately connected with the dynamics of particle production. Another significant aspect about F_q is that an event can contribute to (1) only if $n_m \geq q$. Thus for small δX where $\langle n_m \rangle$ is small in a bin, only rare events with high spikes ($n_m \geq q$) contribute.

If the non-statistical fluctuations are self-similar in nature, in the limit of small bin size, factorial moment follow a power law behaviour like

$$\langle F_q \rangle \propto M^{\alpha_q}$$

i.e.

$$\ln \langle F_q \rangle = \alpha_q \ln M + e\,. \tag{2}$$

This property, in analogy with turbulent fluid dynamics, is called 'intermittency'. α_q measures the strength of the intermittency and is called the intermittency exponent and e is a constant. The intermittency exponents α_q is obtained by performing best fits according to eq. (2).

We have performed our study in one-dimensional η and ϕ space where η, the

pseudo-rapidity is defined in terms of emission angle (θ) as $\eta = -\ln \tan(\theta/2)$ and ϕ is the azimuthal angle with respect to the beam direction. The cosine of emission angle region used is -1 to $+1$. The azimuthal angle region used is 0 to 2π. As shape of this distribution influences the scaling behavior of the factorial moments, we have used the "cumulative" variable. X_η and X_ϕ instead of η and ϕ. The corresponding region of investigation for the variable then become (0, 1). The cumulative variable $X(x)$ is given by the relation as below

$$X(x) = \int_{x_1}^{x} \rho(x')\partial x' \Big/ \int_{x_1}^{x_2} \rho(x')\partial x' \tag{3}$$

where x_1 and x_2 are two extreme points in the distribution $\rho(x)$, between which X varies from 0 to 1. Due to the scale properties of the variables, one particle spectrum stretches in its central region, eliminating the losses from the beam splitting and thus allowing to observe the higher order of moments. In our analysis we will use the above mentioned method [40].

It is possible to correlate the intermittency exponents α_q to the generalized dimensions, by

$$d_q = \alpha_q/(q-1) = 1 - D_q \tag{4}$$

where d_q is the anomalous fractal dimension and measures the intermittency dimension. D_q is the fractal dimension which describes fractal and multifractal in the classical system.

Now non-thermal phase transition λ_q is calculated using the relation

$$\lambda_q = (\alpha_q + 1)/q \tag{5}$$

where α_q is the intermittency exponent. If two different phases are present, then this function should have a minimum at a certain value $q = q_c$.

The multifractal specific heat and entropy :

It is known that some simple thermodynamics approximations could be applicable to the multiparticle production. Bershadskii [41] proposed that the constant specific heat approximation, widely used in the ordinary thermodynamics, may also be applicable to the multifractal data.

If the q dependence of D_q satisfies the condition $D_q > D_{q'}$ for $q < q'$ then the spectra is said to exhibit multifractality and then the multifractal specific heat can be obtained from generalised dimension, D_q by the relation [41]

$$D_q = (a - c) + c\frac{\ln q}{q-1}. \tag{6}$$

Here c is the specific heat and a is some other constant and q can be interpreted

as the inverse of temperature, $q = T^{-1}$ [42]. The entropy parameter is defined by,

$$S = \sum -p(n) \ln p(n) \tag{7}$$

$p(n)$ stands for probability of multiplicity distributions where n is the multiplicity of each events.

5. Results and discussions

In this section, we discuss different findings in a part by part manner.

(1) Analysis of intermittency parameter in pseudorapidity and azimuthal angle space :

To probe the intermittent pattern, we have calculated SFMs of orders 2 to 6 for the bin range from 6 to 60 in pseudorapidity (η) space and azimuthal angle (ϕ) space using eq. (1). The maximum order of the moments is limited by the available statistics in the samples. We have not considered the first few data points M = 2, 3, 4, 5 in order to reduce the effect of momentum conservation which tends to spread the particles in opposite directions and thus reduce the value of factorial moments. This effect becomes weaker as M increases. We transformed the variables to reduce the distortion of intermittency due to non-uniformity of single particle distribution using eq. (3) and performed our analysis with the transformed variables. The scaled factorial moments are calculated in the transformed variables according to eq. (2). In Figures 2(a,b) and 5(a,b) $\ln\langle F_q\rangle$ is plotted as a function of $\ln(M)$ for ring like events and jet like events in η

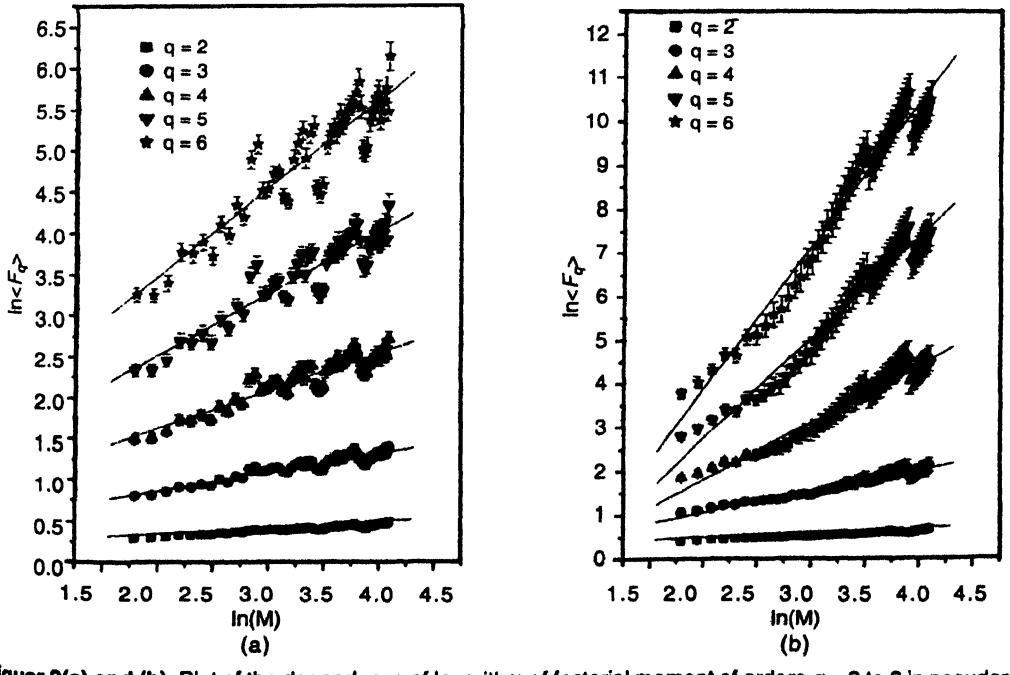

Figuer 2(a) and (b). Plot of the dependence of logarithm of factorial moment of orders q = 2 to 6 in pseudorapidity space (η) for ring like events and jet like events.

and ϕ space. A linear rise of the $\ln\langle F_q\rangle$ with $\ln(M)$ is observed that exhibits the presence of intermittent behavior of particle in each case

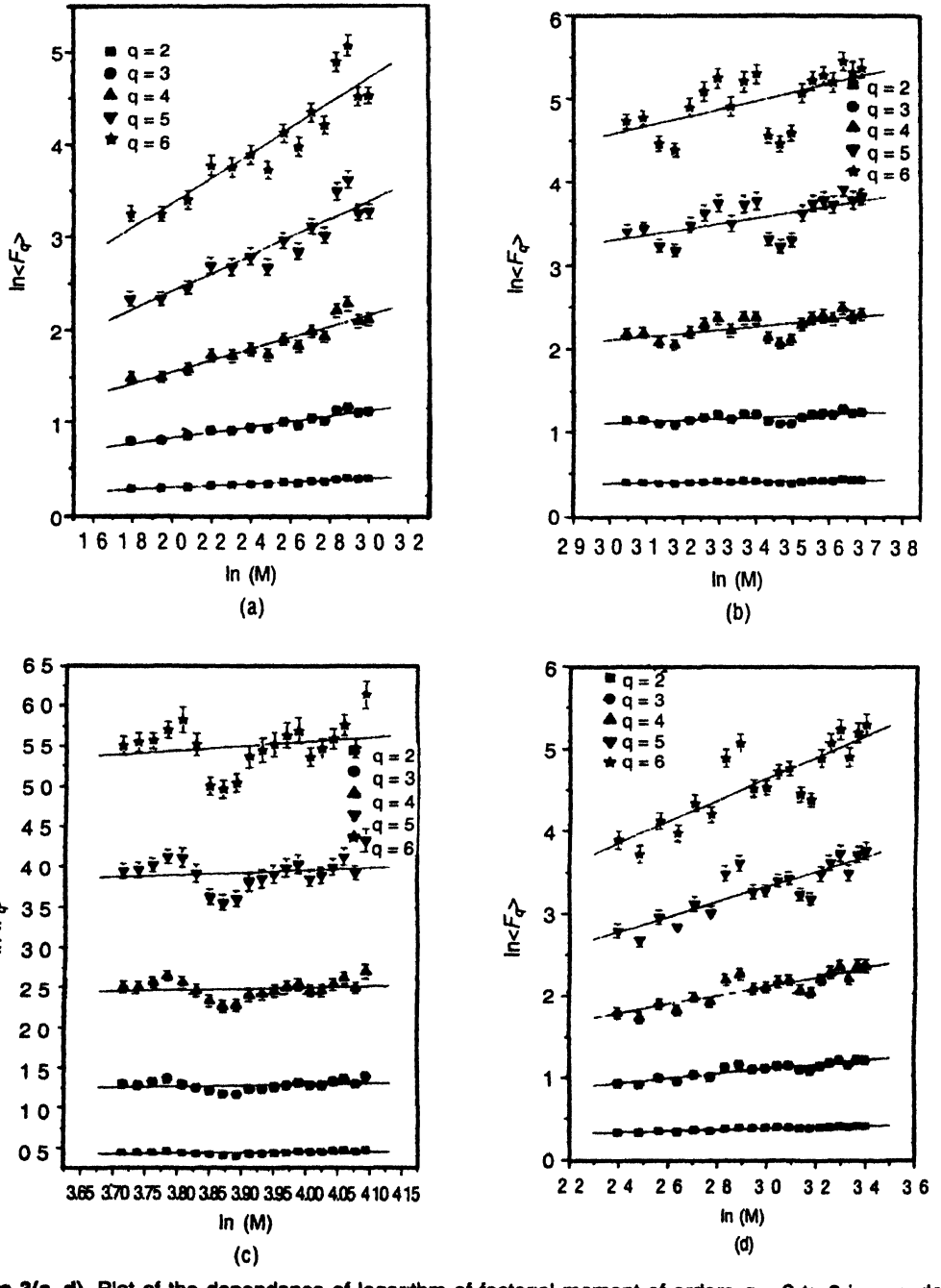

Figure 3(a–d). Plot of the dependance of logarithm of factorial moment of orders $q = 2$ to 6 in pseudorapidity space (η) for ring like events for the bin ranges $6 \leq M \leq 20$, $21 \leq M \leq 40$, $41 \leq M \leq 60$, $11 \leq M \leq 30$, $26 \leq M \leq 45$ respectively.

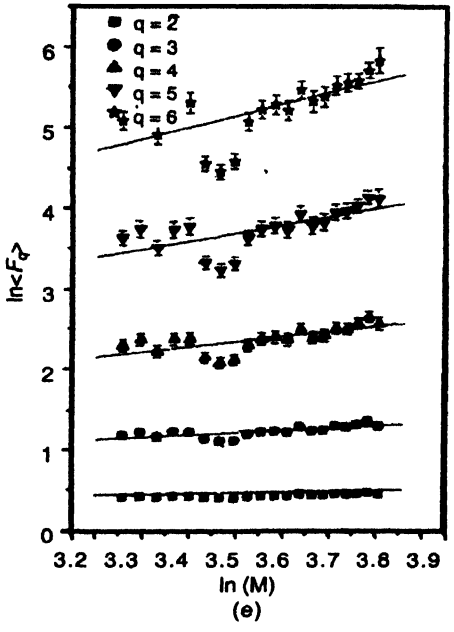

Figure 3(e). Plot of the dependance of logarithm of factorial moment of orders $q = 2$ to 6 in pseudorapidity space (η) for ring like events for the bin ranges $6 \leq M \leq 20$, $21 \leq M \leq 40$, $41 \leq M \leq 60$, $11 \leq M \leq 30$, $26 \leq M \leq 45$ respectively.

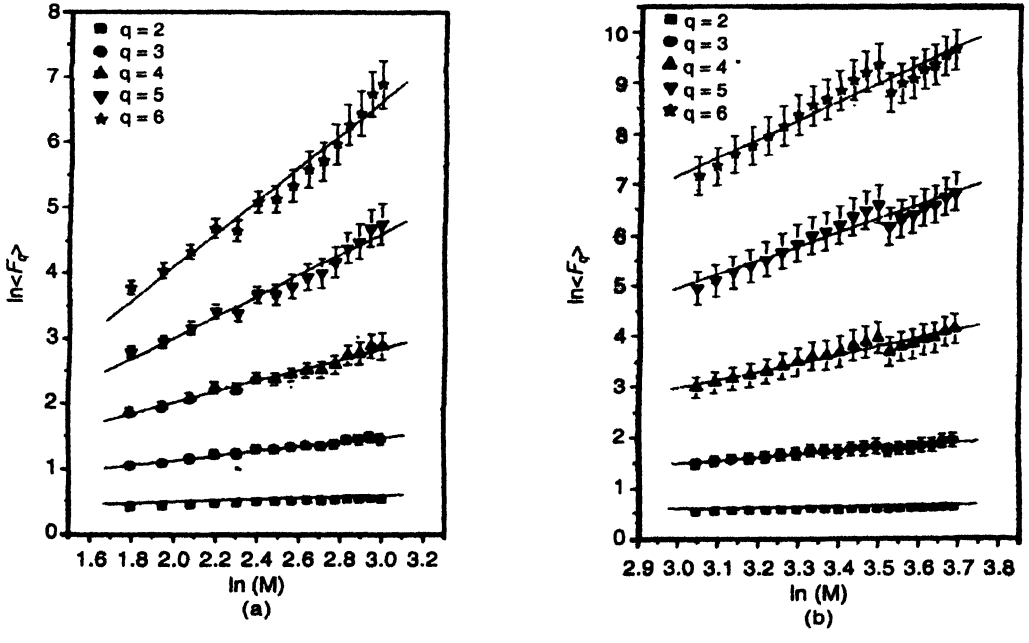

Figure 4(a–b). Plot of the dependance of logarithm of factorial moment of orders $q = 2$ to 6 in pseudorapidity space (η) for jet like events for the bin ranges $6 \leq M \leq 20$, $21 \leq M \leq 40$, $41 \leq M \leq 60$, $11 \leq M \leq 30$, $26 \leq M \leq 45$ respectively

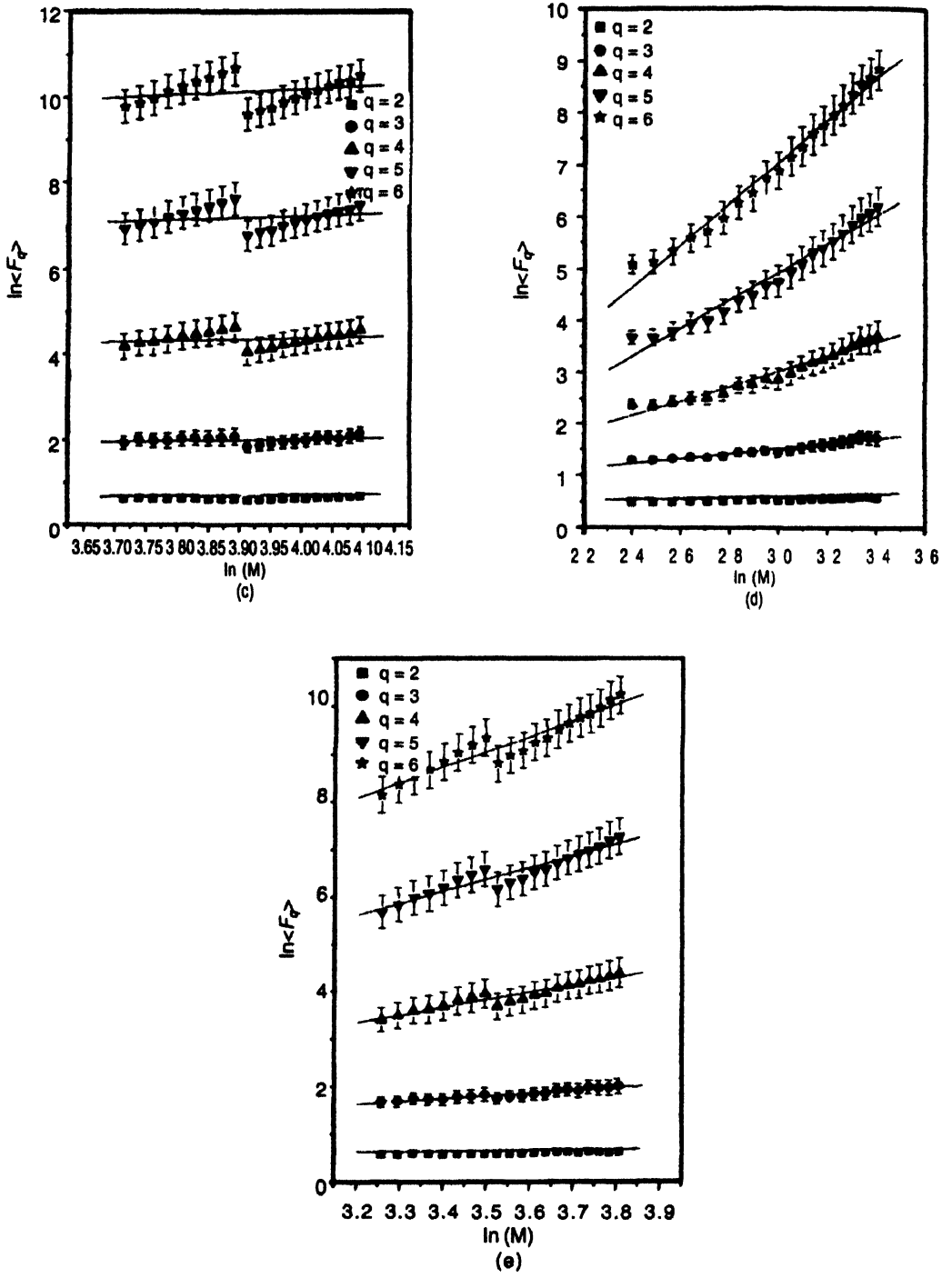

Figure 4(c–e). Plot of the dependance of logarithm of factorial moment of orders $q = 2$ to 6 in pseudorapidity space (η) for jet like events for the bin ranges $6 \leq M \leq 20$, $21 \leq M \leq 40$, $41 \leq M \leq 60$, $11 \leq M \leq 30$, $26 \leq M \leq 45$ respectively

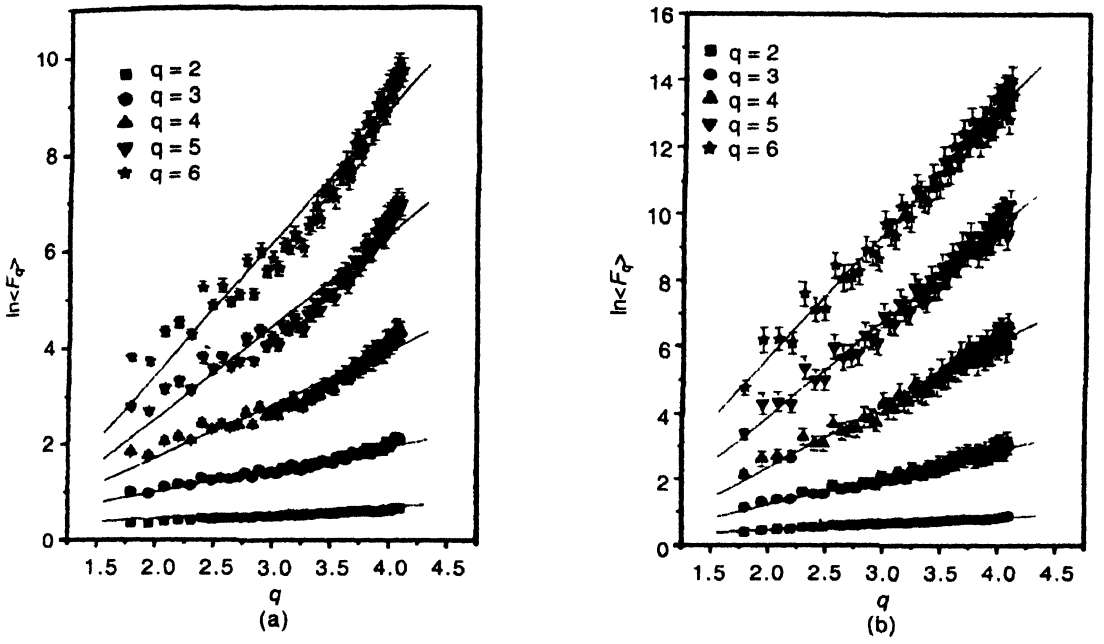

Figure 5(a) and (b). Plot of the dependance of logarithm of factorial moment of orders q = 2 to 6 in azimuthal space (ϕ) for ring like events and jet like events.

To find the best linear behavior for each interaction, linear fit is performed and χ^2 per degrees of freedom are noted. The intermittency exponents α_q are evaluated from linear fitting of the data points according to eq. (2). The values of the intermittency exponent and χ^2 per degrees of freedom for different order of moments for shower multiplicity are shown in Tables 1 and 2 and Tables 5 and 6 for phase space variables η and φ and for the two groups of events respectively.

For variable η the large values of χ^2/DoF (Tables 1 and 2) for ring like and jet like events does not indicate perfect linear fit except for the 2nd order of moment.

Table 1. Values of χ^2/DoF, $\alpha_q(\eta)$ and $\lambda_q(\eta)$ in pseudorapidity (η) space for ring like events.

	$q=2$	$q=3$	$q=4$	$q=5$	$q=6$
χ^2/DoF	0.275	1.060	2.374	4.167	6.551
$\alpha_q(\eta)$	0.073 ± 0.003	0.225 ± 0.011	0.457 ± 0.024	0.746 ± 0.041	1.060 ± 0.059
$\lambda_q(\eta)$	0.536 ± 0.001	0.408 ± 0.003	0.364 ± 0.006	0.349 ± 0.008	0.343 ± 0.009

Table 2. Values of χ^2/DoF, $\alpha_q(\eta)$ and $\lambda_q(\eta)$ in pseudorapidity (η) space for jet like events.

	$q=2$	$q=3$	$q=4$	$q=5$	$q=6$
χ^2/DoF	0.156	0.377	1.317	1.777	1.762
$\alpha_q(\eta)$	0.107 ± 0.003	0.486 ± 0.013	1.313 ± 0.037	2.309 ± 0.060	3.272 ± 0.079
$\lambda_q(\eta)$	0.553 ± 0.001	0.495 ± 0.004	0.576 ± 0.009	0.662 ± 0.012	0.712 ± 0.013

Table 3(a). Values of χ^2/DoF for different bin regions in pseudorapidity (η) space for ring like events.

Bin range	$q=2$	$q=3$	$q=4$	$q=5$	$q=6$
$6 \leq M \leq 20$	0.092	0.596	1.657	3.195	5.109
$21 \leq M \leq 40$	0.238	0.987	2.802	5.186	9.007
$41 \leq M \leq 60$	0.475	1.380	2.444	3.680	30.772
$11 \leq M \leq 30$	0.112	0.696	1.948	3.957	6.878
$26 \leq M \leq 45$	0.296	1.148	2.757	5.161	8.515

Table 3(b). Values of the intermittency exponents $\alpha_q(\eta)$ for different bin regions in pseudorapidity (η) space for ring like events.

Bin range	$q=2$	$q=3$	$q=4$	$q=5$	$q=6$
$6 \leq M \leq 20$	0.088 ± 0.005	0.292 ± 0.025	0.605 ± 0.063	0.973 ± 0.113	1.351 ± 0.167
$21 \leq M \leq 40$	0.058 ± 0.014	0.188 ± 0.053	0.404 ± 0.123	0.694 ± 0.218	1.025 ± 0.331
$41 \leq M \leq 60$	0.080 ± 0.036	0.129 ± 0.112	0.178 ± 0.226	0.317 ± 0.370	0.554 ± 0.541
$11 \leq M \leq 30$	0.085 ± 0.006	0.276 ± 0.029	0.570 ± 0.071	0.925 ± 0.127	1.305 ± 0.191
$26 \leq M \leq 45$	0.095 ± 0.018	0.302 ± 0.068	0.623 ± 0.151	1.013 ± 0.260	1.425 ± 0.388

Table 3(c). Values of $\lambda_q(\eta)$ for different bin regions in pseudorapidity (η) space for ring like events.

Bin range	$q=2$	$q=3$	$q=4$	$q=5$	$q=6$
$6 \leq M \leq 20$	0.544 ± 0.002	0.430 ± 0.008	0.401 ± 0.015	0.394 ± 0.022	0.391 ± 0.027
$21 \leq M \leq 40$	0.527 ± 0.007	0.396 ± 0.017	0.315 ± 0.030	0.338 ± 0.043	0.337 ± 0.055
$41 \leq M \leq 60$	0.540 ± 0.018	0.376 ± 0.037	0.294 ± 0.056	0.263 ± 0.074	0.259 ± 0.090
$11 \leq M \leq 30$	0.542 ± 0.003	0.425 ± 0.009	0.392 ± 0.017	0.385 ± 0.025	0.384 ± 0.031
$26 \leq M \leq 45$	0.547 + 0.009	0.436 ± 0.022	0.405 ± 0.037	0.402 ± 0.052	0.404 ± 0.064

Table 4(a). Values of χ^2/DoF for different bin regions in pseudorapidity (η) space for jet like events.

Bin range	$q=2$	$q=3$	$q=4$	$q=5$	$q=6$
$6 \leq M \leq 20$	0.058	0.109	0.208	0.476	0.830
$21 \leq M \leq 40$	0.078	0.059	0.094	0.172	0.277
$41 \leq M \leq 60$	0.289	0.212	0.290	0.441	0.646
$11 \leq M \leq 30$	0.081	0.228	0.546	0.656	0.583
$26 \leq M \leq 45$	0.091	0.064	0.091	0.145	0.220

Table 4(b). Values of the intermittency exponents $\alpha_q(\eta)$ for different bin regions in pseudorapidity (η) space for jet like events.

Bin range	$q=2$	$q=3$	$q=4$	$q=5$	$q=6$
$6 \leq M \leq 20$	0.102 ± 0.005	0.343 ± 0.014	0.831 ± 0.037	1.598 ± 0.079	2.536 ± 0.
$21 \leq M \leq 40$	0.129 ± 0.010	0.620 ± 0.035	1.652 ± 0.100	2.724 ± 0.172	3.623 ± 0.232
$41 \leq M \leq 60$	0.143 ± 0.038	0.245 ± 0.135	0.327 ± 0.323	0.482 ± 0.474	0.643 ± 0.599
$11 \leq M \leq 30$	0.100 ± 0.007	0.481 ± 0.027	1.423 ± 0.071	2.724 ± 0.108	4.075 ± 0.121
$26 \leq M \leq 45$	0.125 ± 0.014	0.632 ± 0.045	1.617 ± 0.117	2.524 ± 0.188	3.277 ± 0.243

Table 4(c). Values of $\lambda_q(\eta)$ for different bin regions in pseudorapidity (η) space for jet like events.

Bin range	$q=2$	$q=3$	$q=4$	$q=5$	$q=6$
$6 \leq M \leq 20$	0.551 ± 0.002	0.447 ± 0.004	0.457 ± 0.009	0.519 ± 0.015	0.589 ± 0.203
$21 \leq M \leq 40$	0.564 ± 0.005	0.540 ± 0.011	0.663 ± 0.025	0.745 ± 0.034	0.770 ± 0.038
$41 \leq M \leq 60$	0.571 ± 0.019	0.415 ± 0.045	0.331 ± 0.080	0.296 ± 0.094	0.273 ± 0.099
$11 \leq M \leq 30$	0.550 ± 0.003	0.493 ± 0.009	0.604 ± 0.017	0.744 ± 0.021	0.837 ± 0.020
$26 \leq M \leq 45$	0.562 ± 0.007	0.544 ± 0.015	0.654 ± 0.029	0.704 ± 0.037	0.713 ± 0.040

Table 5. Values of χ^2/DoF, $\alpha_q(\phi)$ and $\lambda_q(\phi)$ in azimuthal (ϕ) space for ring like events.

	$q=2$	$q=3$	$q=4$	$q=5$	$q=6$
χ^2/DoF	0.226	0.965	3.341	6.598	9.665
$\alpha_q(\phi)$	0.121 ± 0.003	0.473 ± 0.014	1.119 ± 0.040	1.922 ± 0.069	2.757 ± 0.096
$\lambda_q(\phi)$	0.560 ± 0.001	0.491 ± 0.004	0.529 ± 0.010	0.584 ± 0.013	0.626 ± 0.016

Table 6. Values of χ^2/DoF, $\alpha_q(\phi)$ and $\lambda_q(\phi)$ in azimuthal (ϕ) space for jet like events.

	$q=2$	$q=3$	$q=4$	$q=5$	$q=6$
χ^2/DoF	0.009	0.335	0.490	0.577	0.795
$\alpha_q(\phi)$	0.172 ± 0.003	0.835 ± 0.022	1.892 ± 0.046	2.884 ± 0.062	3.779 ± 0.077
$\lambda_q(\phi)$	0.586 ± 0.001	0.611 ± 0.007	0.723 ± 0.011	0.776 ± 0.012	0.796 ± 0.012

However χ^2/DoF are less than one for ϕ variable only in case of jet like events. Also the χ^2/DoF value, for a particular order of moment, is much better for jet like events, than that for ring like events for both phase space variables. The intermittency exponents, α_q increases gradually with the order of moment, in both ring like and jet like events. From Tables (1 and 2) and Tables (5 and 6) it is observed that for a particular order of moment intermittency exponents for jet like events are significantly larger than those in case of ring like events in both η space and ϕ space. Since the log-log plot does not show perfect linear behaviour, it is necessary to divide the total phase-space into different sub-bin ranges to find out whether the fluctuations show better power law behaviour in different sub-bin ranges, indicating clear signal of intermittency for the two groups of events.

We divided the η and ϕ space into five different bin-ranges ($6 \leq M \leq 20$, $21 \leq M \leq 40$, $41 \leq M \leq 60$, $11 \leq M \leq 30$ and $26 \leq M \leq 45$). Figures 3(a-e), 4(a-e) and Figures 6(a-e), 7(a-e) presents the dependence of ln $\langle F_q \rangle$ on ln M for individual bin range for each order for ring like events and jet like events respectively. The slopes $\alpha_q(\eta)$ and $\alpha_q(\phi)$ for different order of moments for shower multiplicity obtained from the least square fitting of the data points are given in Tables 3(b), 4(b) and Tables 7(b), 8(b). The values of χ^2 per degrees of freedom are presented in Tables 3(a), 4(a) and Tables 7(a), 8(a) for the two groups of events respectively in variables η and ϕ.

The error bars in the figures represent statistical errors. Errors in the measurements

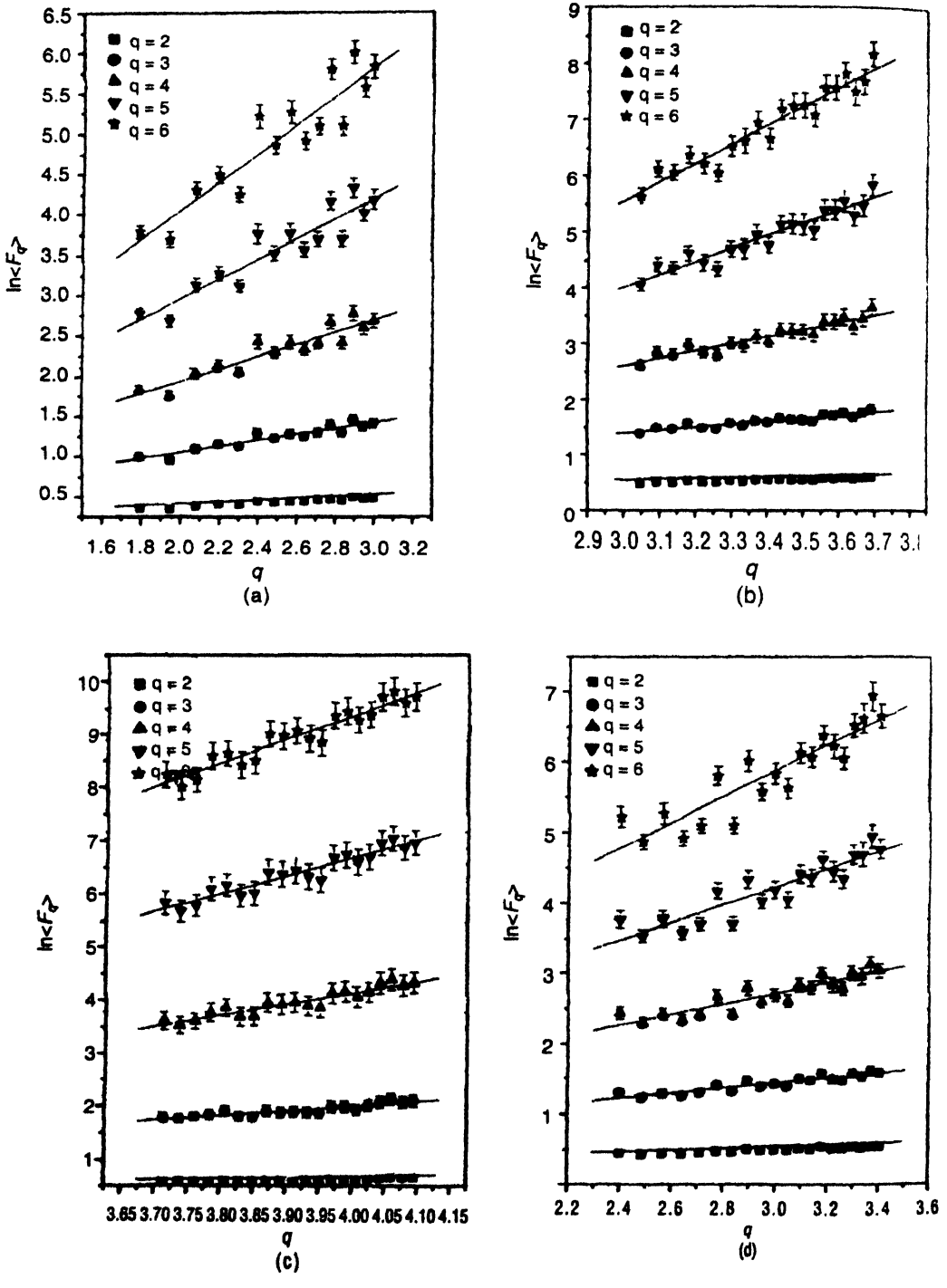

Figure 6(a–d). Plot of the dependance of logarithm of factorial moment of orders $q = 2$ to 6 in pseudorapidity space (ϕ) for ring like events for the bin ranges $6 \leq M \leq 20$, $21 \leq M \leq 40$, $41 \leq M \leq 60$, $11 \leq M \leq 30$, $26 \leq M \leq 45$ respectively.

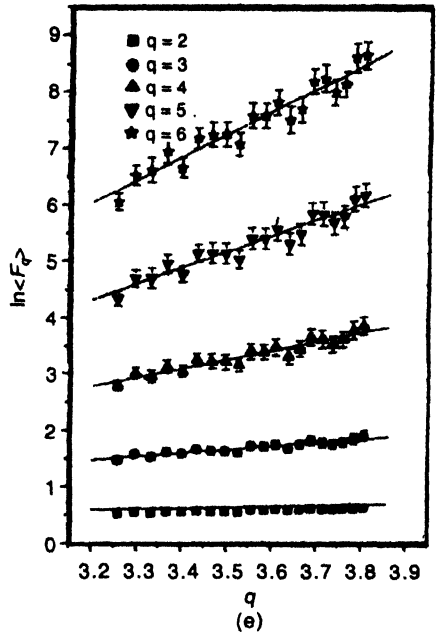

Figure 6(e). Plot of the dependance of logarithm of factorial moment of orders $q = 2$ to 6 in pseudorapidity space (ϕ) for ring like events for the bin ranges $6 \leq M \leq 20$, $21 \leq M \leq 40$, $41 \leq M \leq 60$, $11 \leq M \leq 30$, $26 \leq M \leq 45$ respectively.

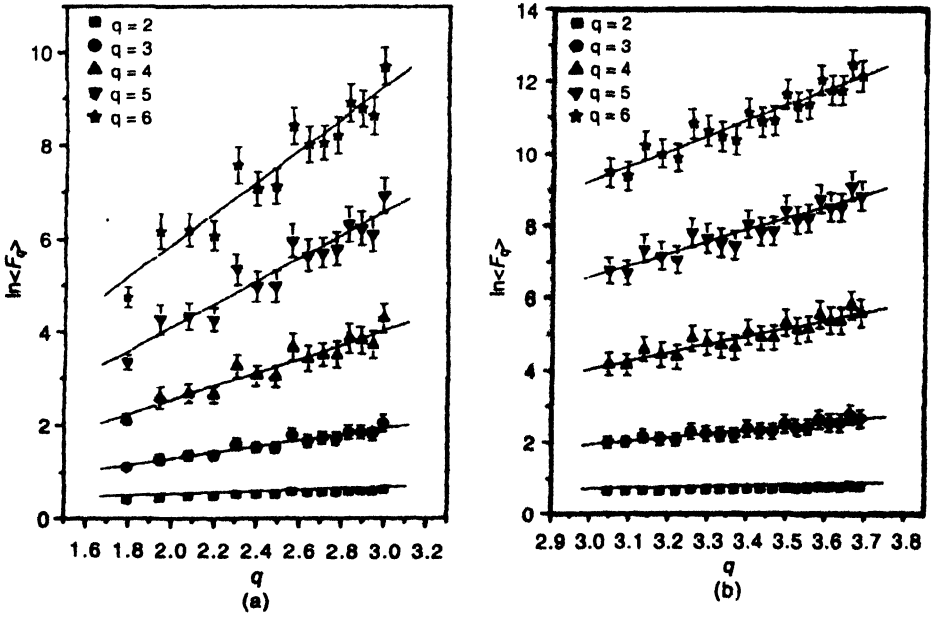

Figure 7(a–b). Plot of the dependance of logarithm of factorial moment of orders $q = 2$ to 6 in azimuthal space (ϕ) for jet like events for the bin ranges $6 \leq M \leq 20$, $21 \leq M \leq 40$, $41 \leq M \leq 60$, $11 \leq M \leq 30$, $26 \leq M \leq 45$ respectively.

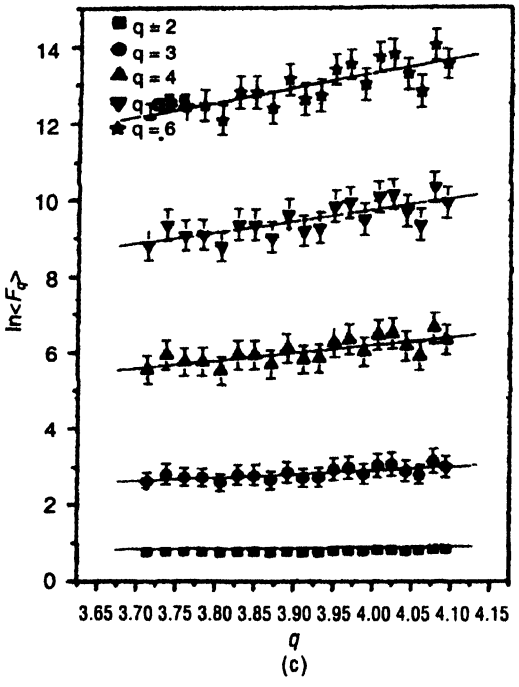

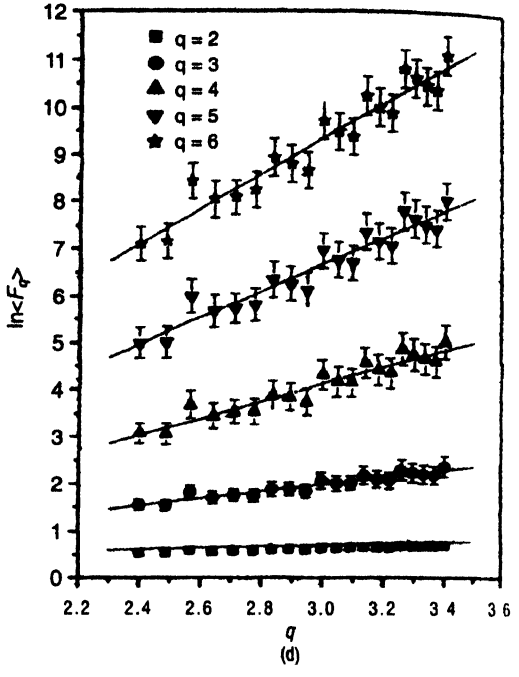

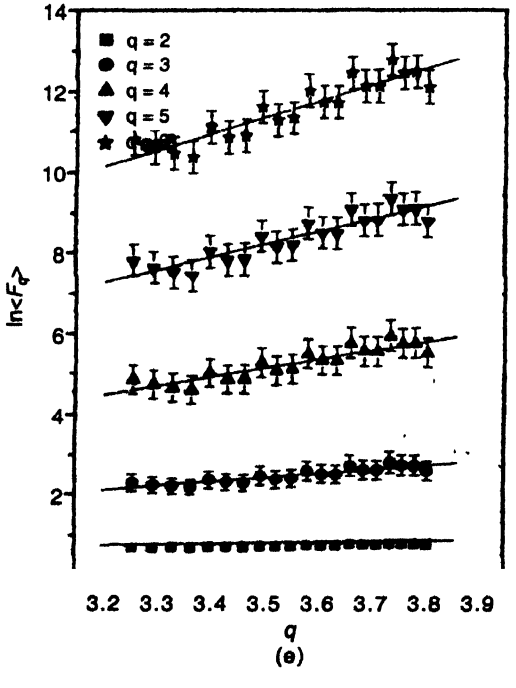

Figure 7(c–e). Plot of the dependance of logarithm of factorial moment of orders $q = 2$ to 6 in azimuthal space (ϕ) for jet like events for the bin ranges $6 \leq M \leq 20$, $21 \leq M \leq 40$, $41 \leq M \leq 60$, $11 \leq M \leq 30$, $26 \leq M \leq 45$ respectively.

Table 7(a). Values of χ^2/DoF for different bin regions in azimuthal (ϕ) space for ring like events.

Bin range	$q=2$	$q=3$	$q=4$	$q=5$	$q=6$
$6 \leq M \leq 20$	0.222	0.947	2.308	4.164	6.254
$21 \leq M \leq 40$	0.158	0.464	0.729	0.966	1.189
$41 \leq M \leq 60$	0.263	0.267	0.263	0.346	0.487
$11 \leq M \leq 30$	0.181	0.720	1.571	2.712	4.103
$26 \leq M \leq 45$	0.102	0.297	0.450	0.615	0.835

Table7(b). Values of the intermittency exponents $\alpha_q(\eta)$ for different bin regions in azimuthal (ϕ) space for ring like events.

Bin range	$q=2$	$q=3$	$q=4$	$q=5$	$q=6$
$6 \leq M \leq 20$	0.122 ± 0.008	0.373 ± 0.033	0.749 ± 0.076	1.217 ± 0.134	1.739 ± 0.198
$21 \leq M \leq 40$	0.125 ± 0.013	0.507 ± 0.049	1.259 ± 0.105	2.351 ± 0.201	3.361 ± 0.222
$41 \leq M \leq 60$	0.188 ± 0.033	0.861 ± 0.093	2.074 ± 0.172	3.337 ± 0.253	4.473 ± 0.330
$11 \leq M \leq 30$	0.107 ± 0.008	0.348 ± 0.034	0.736 ± 0.076	1.243 ± 0.132	1.818 ± 0.196
$26 \leq M \leq 45$	0.142 ± 0.012	0.619 ± 0.048	1.581 ± 0.110	2.800 ± 0.181	4.022 ± 0.251

Table 7(c). Values of $\lambda_q(\phi)$ for different bin regions in azimuthal (ϕ) space for ring like events.

Bin range	$q=2$	$q=3$	$q=4$	$q=5$	$q=6$
$6 \leq M \leq 20$	0.561 ± 0.004	0.458 ± 0.011	0.437 ± 0.019	0.443 ± 0.027	0.456 ± 0.033
$21 \leq M \leq 40$	0.562 ± 0.006	0.502 ± 0.016	0.565 ± 0.026	0.670 ± 0.040	0.727 ± 0.037
$41 \leq M \leq 60$	0.594 ± 0.016	0.620 ± 0.035	0.768 ± 0.043	0.867 ± 0.050	0.912 ± 0.055
$11 \leq M \leq 30$	0.553 ± 0.004	0.449 ± 0.011	0.434 ± 0.019	0.448 ± 0.026	0.468 ± 0.032
$26 \leq M \leq 45$	0.571 ± 0.006	0.539 ± 0.016	0.645 ± 0.027	0.760 ± 0.036	0.837 ± 0.042

Table 8(a). Values of χ^2/DoF for different bin regions is azimuthal (ϕ) spaee for jet like events.

Bin range	$q=2$	$q=3$	$q=4$	$q=5$	$q=6$
$6 \leq M \leq 20$	0.134	0.317	0.552	0.916	1.421
$21 \leq M \leq 40$	0.052	0.126	0.216	0.339	0.495
$41 \leq M \leq 60$	0.108	0.167	0.318	0.514	0.758
$11 \leq M \leq 30$	0.843	0.210	0.335	0 491	0 696
$26 < M < 45$	0.053	0.131	0.234	0.370	0.539

Table 8(b). Values of the intermittency exponents $\alpha_q(\eta)$ for different bin regions in azimuthal (ϕ) space for jet like events.

Bin range	$q=2$	$q=3$	$q=4$	$q=5$	$q=6$
$6 \leq M \leq 20$	0.182 ± 0.011	0.657 ± 0.053	1.502 ± 0.131	2.477 ± 0.214	3.408 ± 0.294
$21 \leq M \leq 40$	0.171 ± 0.015	0.957 ± 0.088	2.189 ± 0.186	3.248 ± 0.261	4.180 ± 0.324
$41 \leq M \leq 60$	0.203 ± 0.043	0.990 ± 0.214	2.030 ± 0.415	2.903 ± 0.557	3.701 ± 0.683
$11 \leq M \leq 30$	0.162 ± 0.010	0.756 ± 0.055	1.807 ± 0.130	2.837 ± 0.193	3.740 ± 0.244
$26 \leq M \leq 45$	0.198 ± 0.018	1.038 ± 0.113	2.194 ± 0.235	3.156 ± 0.334	4.024 ± 0.399

Table 8(c). Values of $\lambda_q(\phi)$ for different bin regions in azimuthal (ϕ) for jet like events in variable (ϕ).

Bin range	$q=2$	$q=3$	$q=4$	$q=5$	$q=6$
$6 \leq M \leq 20$	0.591 ± 0.005	0.552 ± 0.014	0.625 ± 0.032	0.695 ± 0.042	0.735 ± 0.049
$21 \leq M \leq 40$	0.585 ± 0.007	0.652 ± 0.029	0.797 ± 0.046	0.850 ± 0.052	0.863 ± 0.054
$41 \leq M \leq 60$	0.601 ± 0.021	0.663 ± 0.071	0.757 ± 0.103	0.781 ± 0.111	0.784 ± 0.113
$11 \leq M \leq 30$	0.581 ± 0.005	0.585 ± 0.015	0.702 ± 0.032	0.767 ± 0.038	0.790 ± 0.040
$26 \leq M \leq 45$	0.599 ± 0.003	0.679 ± 0.037	0.798 ± 0.058	0.831 ± 0.064	0.834 ± 0.066

of polar angles may be caused due to imperfections like fading of tracks and variation of the shrinkage factor. However, these errors are small and can hardly change the results of this analysis. Thus the uncertainty in the measurement of emission angle does not introduce any appreciable systematic error in our calculations.

Following conclusions for both variables can be drawn from the above analysis.

1) We find from that χ^2 per degrees of freedom values for jet like are much less than one for all orders of moments, indicating perfect linear behavior of ln $\langle F_q \rangle$ with ln M for different sub-bin ranges. These values are much better than the values corresponding to the full range.
2) For ring like events χ^2 per degrees of freedom values are significantly larger than one for all orders except 2nd order.
3) Factorial moments increase with decreasing phase space interval size and the behaviour is compatible with eq. (2).
4) It is evident from the tables that α_q (the strength of intermittency) increases with the order of moments, in case of jet like events as well as ring like events. Intermittency exponents are small particularly for moments of low rank. From the values of intermittency exponents of different sub-bin ranges, we can conclude that different M-intervals show different power-like dependences. Such a behaviour of moments lends support to the existence of distinguished regimes of particle creation at various bin averaging scales.
5) It is interesting to observe that for a particular order q, intermittency exponents for jet like events are significantly larger than those in case of ring like events indicating stronger signal of intermittency in the density fluctuation in both pseudorapidity and azimuthal angle phase space.
6) The slopes $\alpha_q(\phi)$ are higher than those $\alpha_q(\eta)$ values for both ring like and jet like events.

(2) Fractal aspects for ring like and jet like events in both pseudorapidity and azimuthal angle space :

The anomalous fractal dimension d_q and the generalized dimensions D_q are calculated by using eq. (4). These anomalous fractal dimensions describe how the distribution

changes with increasing resolution in the range, where $\alpha_q < q - 1$. In Figures (8–11) the values D_q are plotted against q for the variables (i) η, (ii) ϕ, for full phase space and different M intervals. We observe that

1) d_q values have the tendency to grow almost linearly with the increase in q for all sub-bin ranges for both events, *i.e.* $d_{q1} > d_{q2}$, $q_1 > q_2$. Multifractality observed, as mentioned earlier, points out a cascading scenario of particle production. Multifractality is observed not only in a single bin, but in different bins also. However it is also observed that for a particular order q, anomalous fractal dimension d_q for jet like events, are significantly larger than those in case of ring like events for both variables η and ϕ. Different increase of d_q, with q was found for different intervals, indicating possible change of regime of particle creation.

2) The generalized dimensions D_q decrease gradually with increase of order of moments for both types of events, *i.e.* $D_{q1} < D_{q2}, q_1 > q_2$. It is seen that for a particular order of moment, decrease in the value of D_q is much larger in case of jet like events than that for ring like events.

3) From these figures we observe that $D_q(\phi) < D_q(\eta)$ at all values of q.

(3) Non-thermal phase transition studies :

Further to study the non-thermal phase transition we have calculated λ_q from the values of intermittency exponents α_q according to the eq. (5) for the variable η and ϕ for the two groups of events Tables 1, 2 and Tables 5, 6. From the plots (Figure 12) it is seen

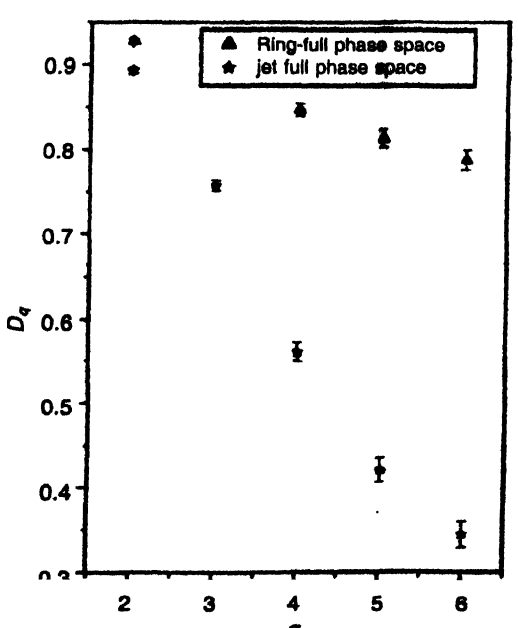

Figure 8. Plot of D_q for different orders q in pseudorapidity space (η) for ring like and jet like events.

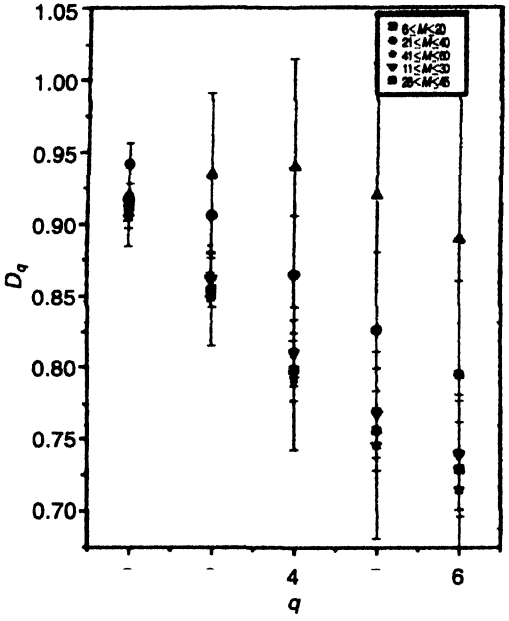

Figure 9(a). Plot of D_q for different bin regions in pseudorapidity space (η) for ring like events.

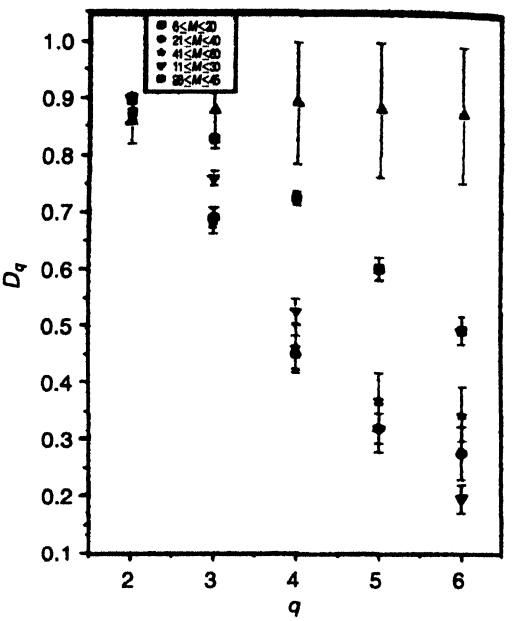

Figure 9(b). Plot of D_q for different bin regions in pseudorapidity space (η) for jet like events.

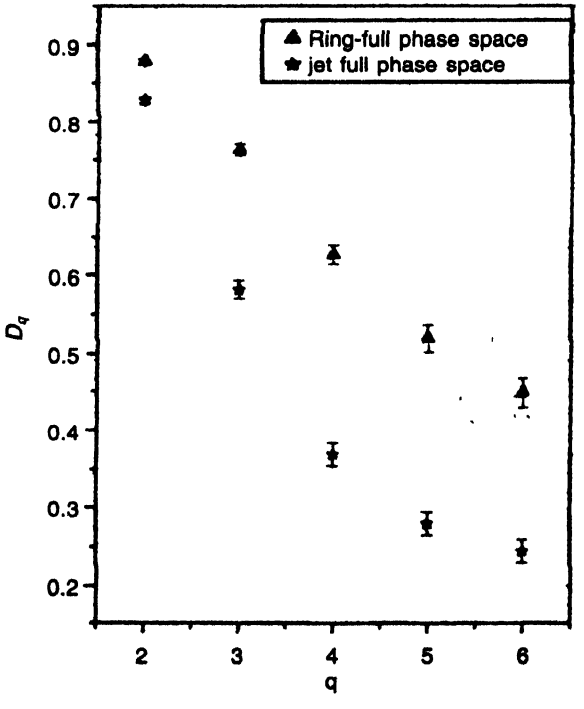

Figure 10. Plot of D_q for different orders q in azimuthal space (ϕ) for ring like jet like events.

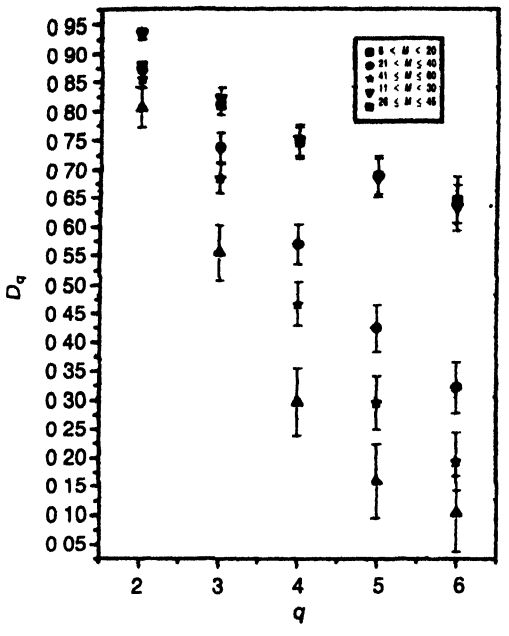

Figure 11(a). Plot of D_q for different bin regions in azimuthal (ϕ) space for ring like events

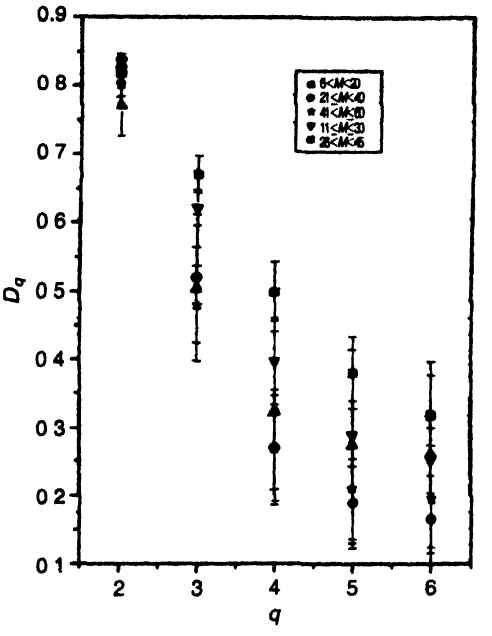

Figure 11(b). Plot of D_q for different bin regions in azimuthal (ϕ) space for jet like events

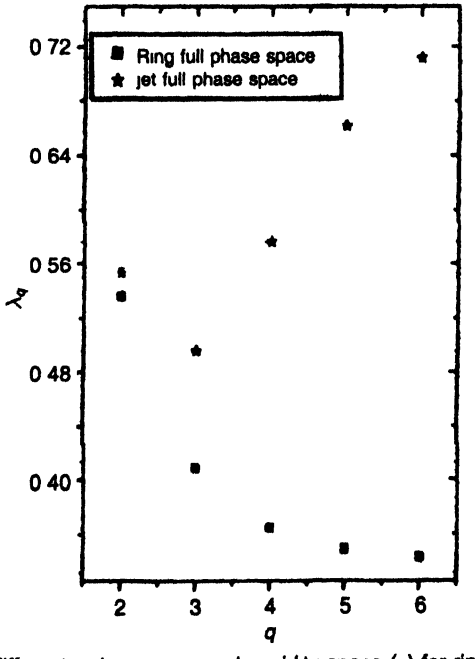

Figure 12. Plot of λ_q for different orders q in pseudorapidity space (η) for ring like and jet like events

that $\lambda_q(\eta)$ shows a clear minimum at $q = 3$ for jet like events. But for the ring like events and $\lambda_q(\eta)$ decreases with order q and no such minimum is obtained. In Figures 14, the same plots are shown for the variable ϕ. $\lambda_q(\phi)$ exhibits an indication of a minimum occurring at $q = 3$ for ring like events. In order to get a clear picture of the phase structure of the multiparticle system, we have studied the non-thermal phase transition in detail for the variable η and ϕ in different sub bins for both jet and ring like events. It is observed from the plots, that,

1) For jet like events minimum $\lambda_q(\eta)$ occurs at $q = 3$ (considering the statistical error at each point) for all the intervals except $41 \leq M \leq 60$. There is a clear indication of a dip and then the $\lambda_q(\eta)$ values start rising and continue up for the higher value of q. As is evident from Figure 13(b), the values are well separated from each other for different bins at the higher order. This occurrence of minimum $\lambda_q(\eta)$ may be attributed to the manifestation of a non-thermal phase transition for the jet like events in the pionisation region of ^{32}S-AgBr interactions at 200 A GeV in variable η.

2) Similarly for ring like events Figure 13(a) reveals the variation of $\lambda_q(\eta)$ with order for different M intervals. It appears from the figure that no minimum of $\lambda_q(\eta)$ occurs for any interval. The values of $\lambda_q(\eta)$ decreases with the order of moment q for all bins.

3) The variation of λ_q as a function of q are shown in Figure 15(b) for the variable ϕ. Jet like events does not show any indication of a minimum value in $\lambda_q(\phi)$.

4) However, for ring like events $\lambda_q(\phi)$ show a minimum (considering the statistical error at each point) for the intervals $21 \leq M \leq 40$ and $26 \leq M \leq 45$ at $q = 3$.

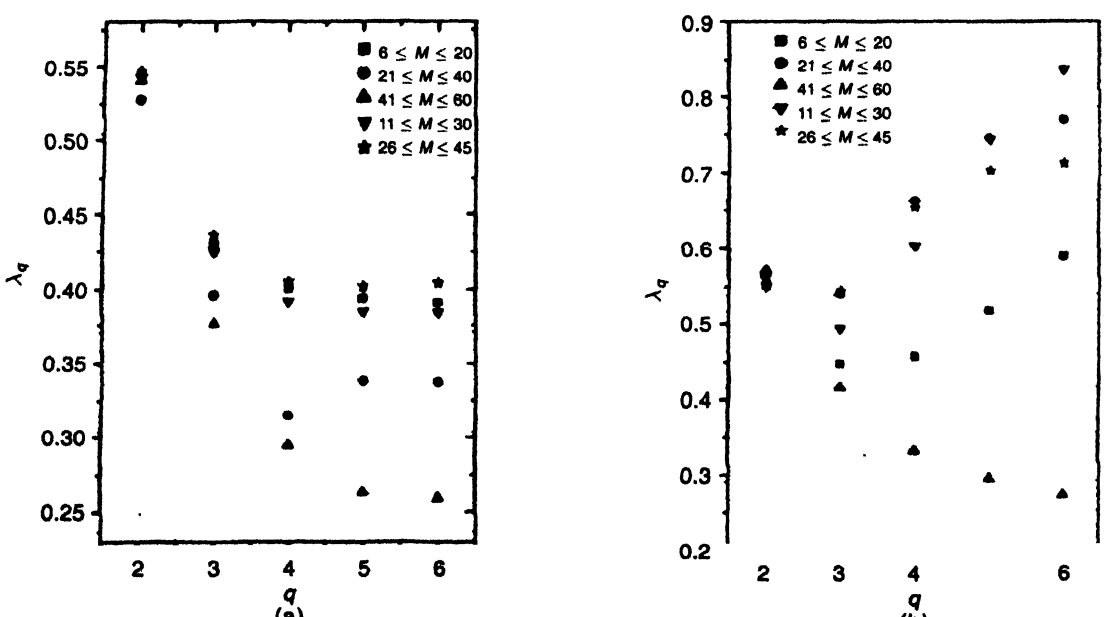

Figure 13(a) and (b). Plot of λ_q for different orders q for different bin regions in pseudorapidity space (η) for ring like and jet like events.

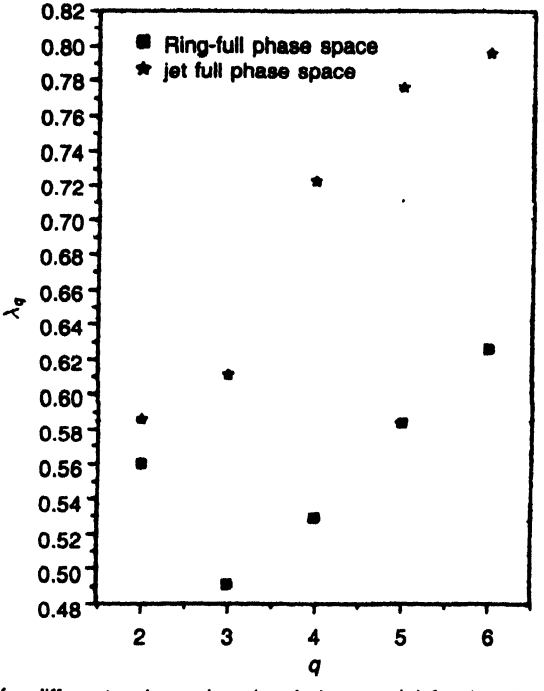

Figure 14. Plot of λ_q for different orders q in azimuthal space (ϕ) for ring like and jet like events.

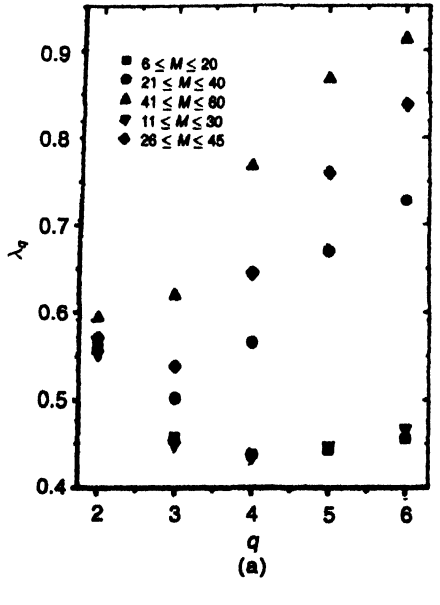

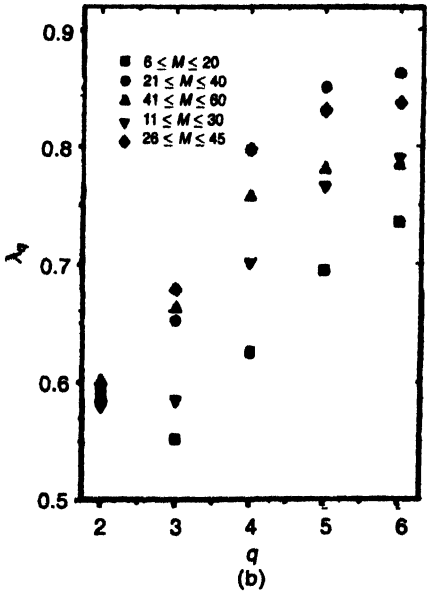

Figure 15(a) and (b). Plot of λ_q for different orders q for different bin regions in azimuthal space (ϕ) for ring like and jet like events.

6. Multifractal specific heat and entropy

To extract the specific heat, the values of the generalized dimensions D_q are plotted as a function of $\ln q/(q-1)$. Figures 16–19 show the graphs for ring like and jet like events in variables η and ϕ. The slopes of the best linear fits of the data sets of the figures give the values of the specific heat c which are tabulated in Table 15. The table shows that for both events, specific heats are different in different bin ranges. Entropy of total events and jet like events are given in Table 16.

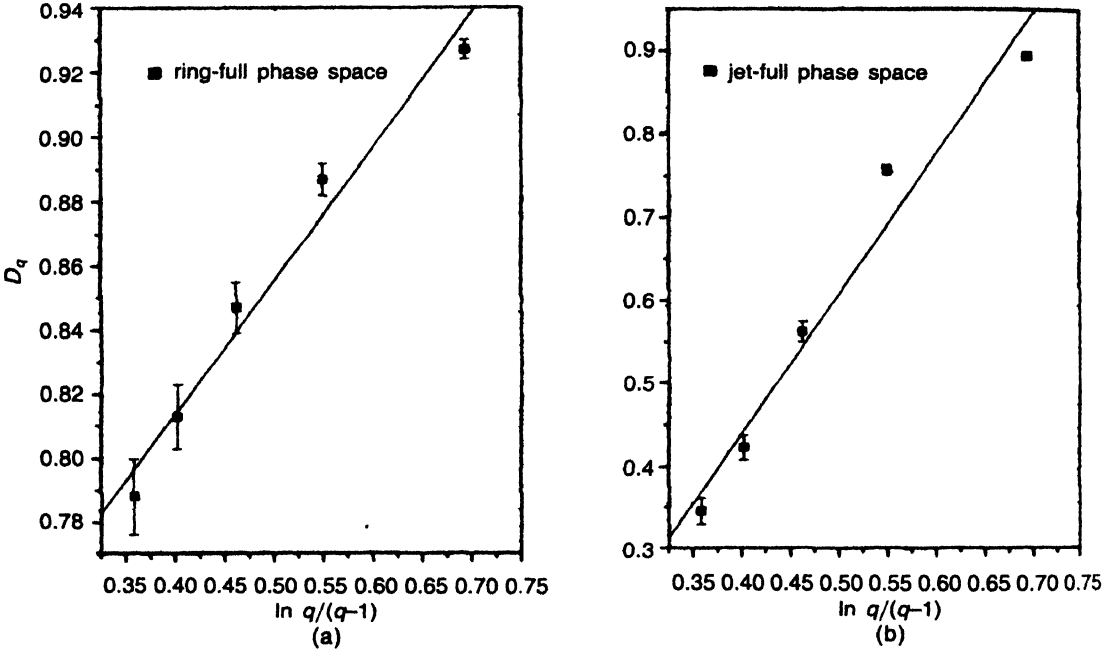

Figure 16(a and b). Plot of D_q against ln $q/(q-1)$ in pseudorapidity (η) space for ring like and jet like events

7. Conclusions and summary

In this paper we have made an attempt to study the dynamics of fluctuations and fractality in the multiparticle production in ^{32}S-AgBr interaction at 200 A GeV for ring like and jet like events separately. Since, the analysis in one phase space (η) can give restricted information of the fluctuation pattern of the emission process, it is essential to study in other phase space, *i.e.* in the azimuthal angle space (ϕ) also, to have a better visibility of the significance of the multifractal nature of the produced pions for both type of events. Let us conclude the whole findings in this study of ^{32}S-AgBr interactions at 200 A GeV for ring like and jet like events in the following manner.

a) Our results show strong signal of intermittency only in jet like events for both the variables η and ϕ.

It is difficult to justify theoretically the observed fluctuation in ring like and jet like events, since there is no model till date which can explain ring like events. One of the

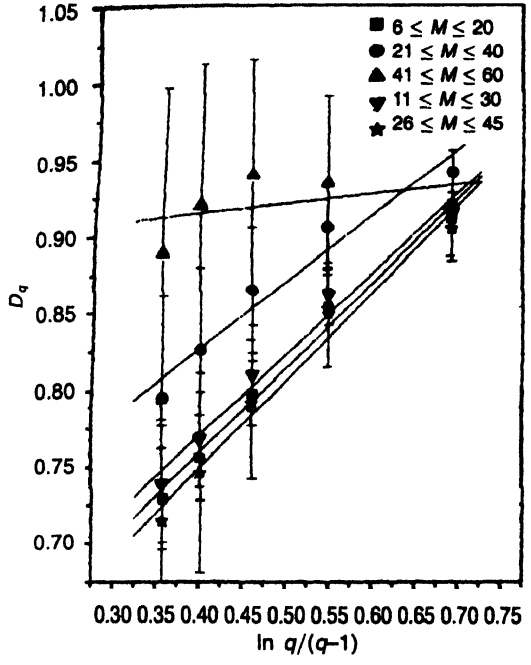

Figure 17a. Plot of D_q against ln $q/(q-1)$ in different bin regions in (η) space for ring like events.

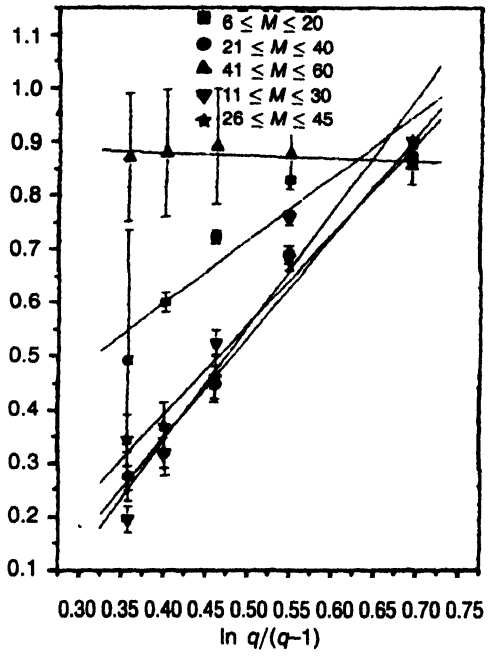

Figure 17b. Plot of D_q against ln $q/(q-1)$ in different bin regions in (η) space for jet like events.

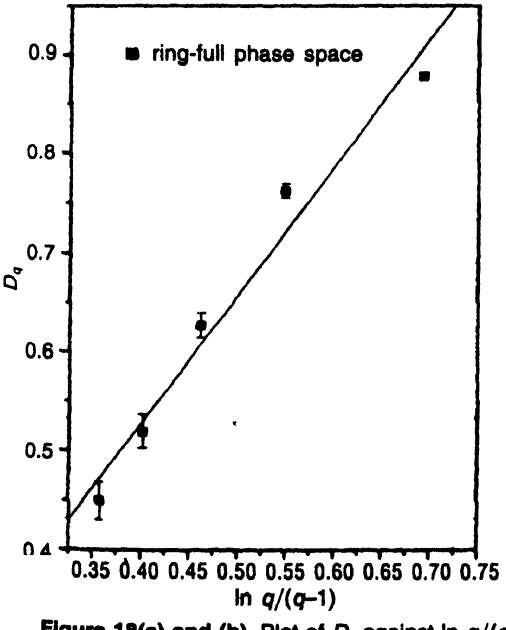

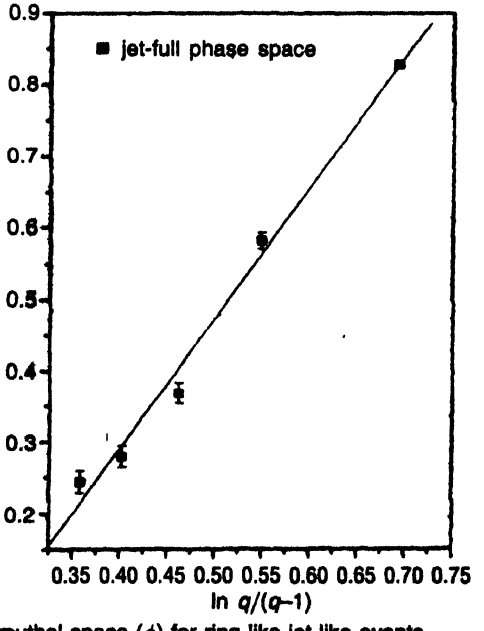

Figure 18(a) and (b). Plot of D_q against ln $q/(q-1)$ in azimuthal space (ϕ) for ring like jet like events.

suggestions [29,31–38] of the origin of the so-called ring-like events is the possible formation of Cherenkov gluon radiation in analogy to Cherenkov electromagnetic radiation.

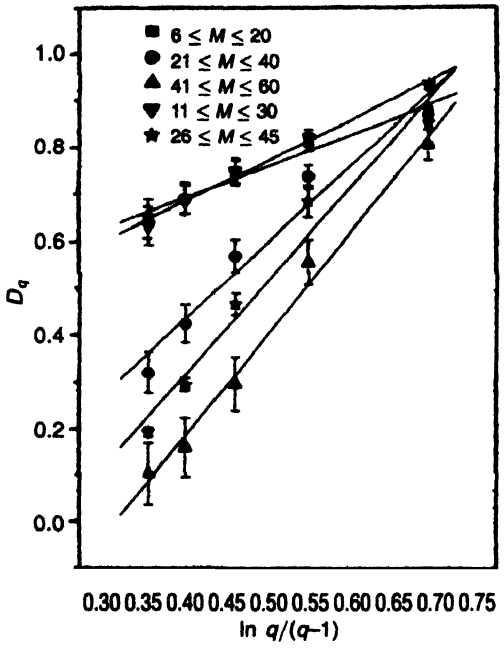

Figure 19(a). Plot of D_q against ln $q/(q-1)$ for different bin regions (ϕ) space for ring like events.

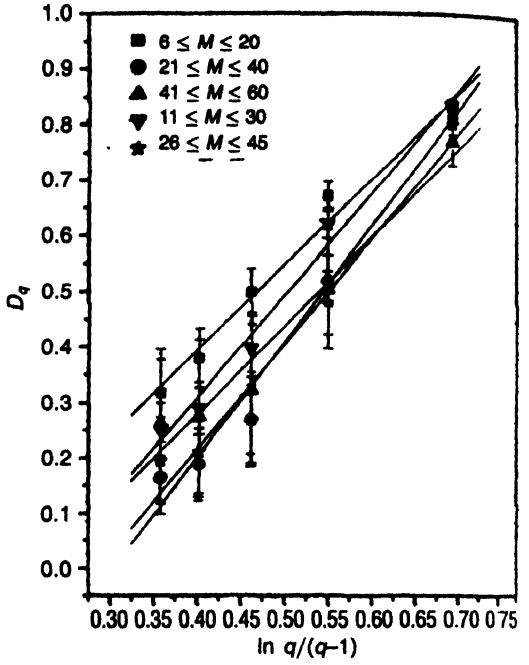

Figure 19(b). Plot of D_q against ln $q/(q-1)$ for different bin regions (ϕ) space for ring like events

Table 9. Values of $d_q(\eta)$ and $D_q(\eta)$ in pseudorapidity (η) space for ring like events.

	$q=2$	$q=3$	$q=4$	$q=5$	$q=6$
$d_q(\eta)$	0.073	0.112	0.152	0.186	0.212
$D_q(\eta)$	0.927	0.887	0.847	0.813	0.788
	± 0.003	± 0.005	± 0.008	± 0.010	± 0.012

Table 10. Values of $d_q(\eta)$ and $D_q(\eta)$ in pseudorapidity (η) space for jet like events.

	$q=2$	$q=3$	$q=4$	$q=5$	$q=6$
$d_q(\eta)$	0.107	0.243	0.437	0.577	0.654
$D_q(\eta)$	0.893	0.757	0.562	0.422	0.345
	± 0.003	± 0.006	± 0.012	± 0.015	± 0.016

Cherenkov-gluons will be emitted by a parton (quark) entering a hadronic medium at the cone surface with the cone angle θ in the rest system of the infinite medium defined by the relation

$$\cos\theta = 1/\beta n$$

where β is the ratio of the velocities of the parton-emitter and light. Each gluon would produce a jet. These jets should form the ring with jetty" substructure (spots) in the azimuthal plane perpendicular to the direction of the primary parton. The necessary

Table 11(a). Values of $d_q(\eta)$ and $D_q(\eta)$ for different bin regions in pseudorapidity (η) space for ring like events.

Bin range		$q=2$	$q=3$	$q=4$	$q=5$	$q=6$
$6 \leq M \leq 20$	$d_q(\eta)$	0.088	0.146	0.201	0.243	0.270
	$D_q(\eta)$	0.912 ± 0.005	0.854 ± 0.012	0.798 ± 0.021	0.756 ± 0.028	0.729 ± 0.033
$21 \leq M \leq 40$	$d_q(\eta)$	0.058	0.094	0.134	0.173	0.205
	$D_q(\eta)$	0.942 ± 0.014	0.906 ± 0.026	0.865 ± 0.041	0.826 ± 0.054	0.795 ± 0.066
$41 \leq M \leq 60$	$d_q(\eta)$	0.080	0.064	0.059	0.079	0.110
	$D_q(\eta)$	0.920 ± 0.036	0.935 ± 0.056	0.940 ± 0.075	0.920 ± 0.092	0.889 ± 0.108
$11 \leq M \leq 30$	$d_q(\eta)$	0.085	0.138	0.190	0.231	0.261
	$D_q(\eta)$	0.915 ± 0.006	0.862 ± 0.014	0.810 ± 0.023	0.768 ± 0.031	0.739 ± 0.038
$26 \leq M \leq 45$	$d_q(\eta)$	0.095	0.151	0.207	0.253	0.285
	$D_q(\eta)$	0.905 ± 0.018	0.849 ± 0.034	0.792 ± 0.050	0.746 ± 0.065	0.715 ± 0.077

Table 11(b). Values of $d_q(\eta)$ and $D_q(\eta)$ for different bin regions in pseudorapidity (η) space for jet like events.

Bin range		$q=2$	$q=3$	$q=4$	$q=5$	$q=6$
$6 \leq M \leq 20$	$d_q(\eta)$	0.102	0.171	0.277	0.399	0.507
	$D_q(\eta)$	0.898 ± 0.005	0.828 ± 0.007	0.723 ± 0.012	0.600 ± 0.019	0.492 ± 0.024
$21 \leq M \leq 40$	$d_q(\eta)$	0.129	0.310	0.550	0.681	0.724
	$D_q(\eta)$	0.871 ± 0.010	0.690 ± 0.017	0.449 ± 0.033	0.319 ± 0.043	0.275 ± 0.046
$41 \leq M \leq 60$	$d_q(\eta)$	0.143	0.122	0.109	0.120	0.128
	$D_q(\eta)$	0.857 ± 0.038	0.877 ± 0.067	0.891 ± 0.107	0.879 ± 0.118	0.871 ± 0.119
$11 \leq M \leq 30$	$d_q(\eta)$	0.100	0.240	0.474	0.681	0.805
	$D_q(\eta)$	0.900 ± 0.007	0.759 ± 0.013	0.525 ± 0.023	0.319 ± 0.027	0.195 ± 0.024
$26 \leq M \leq 45$	$d_q(\eta)$	0.125	0.316	0.539	0.631	0.655
	$D_q(\eta)$	0.875 ± 0.014	0.684 ± 0.022	0.461 ± 0.039	0.369 ± 0.047	0.344 ± 0.048

Table 12. Values of $d_q(\phi)$ and $D_q(\phi)$ in azimuthal (ϕ) space for ring like events.

	$q=2$	$q=3$	$q=4$	$q=5$	$q=6$
$d_q(\phi)$	0.121	0.236	0.373	0.480	0.551
$D_q(\phi)$	0.879 ± 0.003	0.763 ± 0.007	0.627 ± 0.013	0.519 ± 0.017	0.449 ± 0 019

Table 13. Values of $d_q(\phi)$ and $D_q(\phi)$ in azimuthal (ϕ) space for jet like events.

	$q=2$	$q=3$	$q=4$	$q=5$	$q=6$
$d_q(\phi)$	0.172	0.417	0.630	0.721	0.755
$D_q(\phi)$	0.828 ± 0.003	0.582 ± 0.011	0.369 ± 0.015	0.279 ± 0.015	0.244 ± 0.015

Table 14(a). Values of $d_q(\phi)$ and $D_q(\phi)$ for different bin regions in azimuthal (ϕ) space for ring like events.

Bin range		$q=2$	$q=3$	$q=4$	$q=5$	$q=6$
$6 \leq M \leq 20$	$d_q(\phi)$	0.123	0.189	0.254	0.310	0.353
	$D_q(\phi)$	0.879 ± 0.009	0.810 ± 0.017	0.745 ± 0.026	0.690 ± 0.034	0.647 ± 0.041
$21 \leq M \leq 40$	$d_q(\phi)$	0.130	0.263	0.431	0.576	0.679
	$D_q(\phi)$	0.870 ± 0.014	0.737 ± 0.025	0.569 ± 0.035	0.424 ± 0.041	0.321 ± 0.044
$41 \leq M \leq 60$	$d_q(\phi)$	0.195	0.444	0.703	0.840	0.897
	$D_q(\phi)$	0.805 ± 0.034	0.555 ± 0.048	0.296 ± 0.058	0.159 ± 0.064	0.103 ± 0.066
$11 \leq M \leq 30$	$d_q(\phi)$	0.108	0.177	0.249	0.314	0.366
	$D_q(\phi)$	0.933 ± 0.009	0.822 ± 0.017	0.750 ± 0.026	0.685 ± 0.034	0.633 ± 0.040
$26 \leq M \leq 45$	$d_q(\phi)$	0.146	0.316	0.534	0.704	0.807
	$D_q(\phi)$	0.854 ± 0.013	0.684 ± 0.026	0.466 ± 0.038	0.295 ± 0.046	0.193 ± 0.051

condition for this effect is the excess of the real part of the index of refraction over 1.

b) The behaviour of the generalized dimensions reflects the multifractal behaviour in multiparticle production for both events.

c) The dynamical nature of multifractal structure indicates possible non-thermal phase transition. The pattern of $\lambda_q(\eta)$ against q shows a clear evidence of non-thermal phase transition for jet like events in η. In case of ϕ variable there is an indication of non-thermal phase transition in case of ring like events.

d) Finally it is observed that multifractal specific heats calculated for the two events

Table 14(b). Values of $d_q(\phi)$ and $D_q(\phi)$ for different bin regions in azimuthal (ϕ) space for jet like events.

Bin range		$q=2$	$q=3$	$q=4$	$q=5$	$q=6$
$6 \leq M \leq 20$	$d_q(\phi)$	0.182	0.328	0.500	0.619	0.682
	$D_q(\phi)$	0.818 ± 0.011	0.671 ± 0.026	0.499 ± 0.043	0.380 ± 0.053	0.318 ± 0.059
$21 \leq M \leq 40$	$d_q(\phi)$	0.172	0.479	0.729	0.812	0.836
	$D_q(\phi)$	0.828 ± 0.012	0.520 ± 0.044	0.270 ± 0.062	0.188 ± 0.065	0.164 ± 0.065
$41 \leq M \leq 60$	$d_q(\phi)$	0.203	0.495	0.677	0.725	0.740
	$D_q(\phi)$	0.770 ± 0.043	0.504 ± 0.107	0.323 ± 0.138	0.274 ± 0.139	0.260 ± 0.136
$11 \leq M \leq 30$	$d_q(\phi)$	0.163	0.377	0.602	0.709	0.748
	$D_q(\phi)$	0.837 ± 0.010	0.622 ± 0.027	0.397 ± 0.043	0.290 ± 0.048	0.252 ± 0.048
$26 \leq M \leq 45$	$d_q(\phi)$	0.198	0.520	0.731	0.789	0.805
	$D_q(\phi)$	0.802 ± 0.019	0.480 ± 0.057	0.268 ± 0.078	0.211 ± 0.081	0.195 ± 0.079

Table 15. The multifractal specific heat in η-space and ϕ-space.

		η-Space	ϕ-Space
Ring like events	Full phase space	0.415 ± 0.039	1.301 ± 0.131
	$6 \leq M \leq 20$	0.553 ± 0.039	0.684 ± 0.064
	$21 \leq M \leq 40$	0.434 ± 0.056	1.647 ± 0.201
	$41 \leq M \leq 60$	0.062 ± 0.078	2.194 ± 0.136
	$11 \leq M \leq 30$	0.528 ± 0.044	0.833 ± 0.046
	$26 \leq M \leq 45$	0.571 ± 0.049	2.015 ± 0.217
Jet like events	Full phase space	1.688 ± 0.186	1.825 ± 0.128
	$6 \leq M \leq 20$	1.179 ± 0.226	1.540 ± 0.128
	$21 \leq M \leq 40$	1.887 ± 0.167	2.089 ± 0.179
	$41 \leq M \leq 60$	−0.054 ± 0.044	1.595 ± 0.169
	$11 \leq M \leq 30$	2.144 ± 0.314	1.841 ± 0.123
	$26 \leq M \leq 45$	1.693 ± 0.141	1.895 ± 0.207

Table 16. The entropy parameter for total and jet like events.

Entropy	Total events	Jet like events
	2.639	2.20

are different in different bin ranges.

Acknowledgments

One of the authors, SGR, acknowledges the University Grants Commission, Government of India of its assistance through the Faculty Improvement Programme.

References

[1] T H Burnet *et al, JACEE Collaboration, Phys. Rev. Lett* **50** 2060 (1983)

[2] E A De Wolf, I M Dremin and W Kittel *Physics Reports* **270** (1996)

[3] A Bialas and R Peschanski *Nucl. Phys.* **B273** 703 (1986)

[4] R Peschanski *Int. J. Mod. Phys.* **A6** 3681 (1991)

[5] A Bialas *Nucl. Phys.* **A525** 345c (1991); *ibid* **A545** 285c (1992)

[6] P L Jain and G Singh *Nucl. Phys.* **A596** 700 (1996)

[7] P Lipand and P Buschbuk *Phys. Lett.* **B223** 465 (1990)

[8] N M Agababyan *et al, Phys. Lett.* **B431** 451 (1998)

[9] N M Agababyan *et al, Phys. Lett.* **B382** 305 (1996)

[10] M M Smolarleiewicz *et al, Acta Physica Polonica* **B31** 385 (2000)

[11] D Ghosh *et al, Phys. Rev.* **C58** 3553 (1998)

[12] A M Tawfik *J. Phys.* **G27** 2283 (2001)

[13] R Holynsky *et al,* (KLM Collaboration) *Phys. Rev. Lett.* **62** 733 (1989); *Phys. Rev.* **C40** R2449 (1989)

[14] W Braunschweig *et al,* (TASSO Collaboration), *Phys. Lett.* **B231** 548 (1989)

[15] C Albajar *et al,* (UA1 Collaboration), *Nucl. Phys.* **B345** 1 (1990)

[16] B B Mandelbrot in *Dynamics of Fractal Surfaces* (eds.) E Family and T Viesek (Singapore : World Scientific) (1991); *The Fractal Geometry of Nature* (New York : Freeman) (1982)

[17] H G E Hantschel and I Procaceia *Physica* **D8** 435 (1983)

[18] G Paladin and A Valpiani *Phys. Rep.* **156** 147 (1987)

[19] P Lipa and B Buschbeck *Phys. Lett.* **B233** 465 (1989)

[20] E K Sarkisyan, L K Gelvani, G I Gogiberidze and G G Taran *Phys. Lett.* **B347** 439 (1995); D Ghosh *et al, Z. Phys.* **C71** 243 (1996)

[21] A Bialas and R C Hwa *Phys. Lett.* **B253** 436 (1991)

[22] R Peschanski *Nucl. Phys.* **B327** 144 (1989)

[23] M Adamovich *et al, J. Phys.* **G19** 2035 (1993)

[24] A B Aponasenka *et al, Pis'ma Zh. Eksp. Teor.* **Flz30** 157 (1979)

[25] A V Aponascnka, N A Dobrotin and I M Dremin *et al, JETP Lett.* **30** 145 (1979)

[26] K I Alexeeva *et al, Izvestia AN SSSR* **26** 572 (1962); *J. Phys. Soc. Japan* **17,A-III** 409 (1962)

[27] N V Maslennikova *et al, Izvestia AN SSSR* **36** 1696 (1972)

[28] N Arata *Nuovo Cimento* **43A** 455 (1978)

[29] I M Dremin *et al, JETP Lett.* **40** 320 (1984); *Proc. 17th ICREC* **5** 149 (1981)

[30] A El-Naghy *et al, Phys. Lett.* **B299** 370 (1993)

[31] I A Marutyan *et al, Yad Fiz* **29** 1556 (1979)

[32] M Adamus *et al*, (NA22 Collaboration) *J. Phys.* **G19** 200 (1993)

[33] I M Dremin *JETP Lett.* **30** 140 (1979a)

[34] I M Dremin *SoV. J. Nucl. Phys.* **33** 726 (1981a)

[35] I M Dremin *JETP Lett.* **34** 595 (1981b)

[36] I M Dremin *SoV. J. Nucl. Phys.* **37** 387 (1983)

[37] I M Dremin *Nucl. Phys.* **A767** 233 (2006) and refs. therein

[38] I M Dremin, L I Sarycheva and K Yu Teplov *Eur. Phys. J.* **C46** 429 (2006); I M Dremin hep-ph/0612170 (2006)

[39] A Bialas and R Peschanski *Nucl. Phys.* **B308** 857 (1988)

[40] W Ochs *Z. Phys.* **C50** 339 (1991)

[41] A Bershadskii *Eur. Phys. J.* **A2** 223 (1998)

[42] V Simak *et al*, *Phys. Lett.* **B206** 159 (1988)